Faculty of Engineering, Built Environment and Information Technology

Data Driven automatic damage detection model for cantilevered beam

MRN 422 Final Report

Inkanyezi Pascal
170555459

Executive summary

Structural health monitoring plays an important role in monitoring the integrity and performance of structures. Non-destructive techniques such as vibration-based monitoring help to optimise structural health monitoring, however, requires a large amount of data to be analysed. This presents the need for data-driven vibration-based monitoring systems and anomaly detection offer a solution. This study looks at developing a data-driven vibration-based monitoring technique that utilises anomaly detection to detect damage in cantilevered beams. The method utilises the effect of damage on the vibrational characteristics of a structure and combines this data with anomaly detection machine learning algorithms (more specifically) a semi-supervised machine learning algorithm. The method aims to be able to detect edge cracks in a cantilevered beam based on the vibrational data of the beam and then reveal the progression of the crack. This report covers relevant theory which will be used to build this method such as the compliance method and perturbation method, data-driven models such as anomaly detection (including machine learning) as well as offering background on how vibration works. The model utilised is a PCA autoencoder, the autoencoder has a 78% performance when trained using the natural frequencies of a beam at 1% and performs at 100% when trained using FRF data of a cantilevered beam. Crack progression method is also presented which uses interpolation to determine the extent of damage in the structure.

RPP Compliance matrix

Requirement	**Proposal**		**Project report**	
	Section	**Page**	**Section**	**Page**
Literature review	Objective and Scope	1	2	7
Numerical investigation	Objective and Scope	3-4	3	22
Experimental investigation	Objective and Scope	4	4	32
Crack progression model	Objective and scope	5	5	41

Table of Contents

Executive summary ..... **i**

RPP Compliance matrix ..... **ii**

Table of Contents ..... **iii**

List of Figures ..... **iv**

List of Tables ..... **iv**

List of Symbols ..... **v**

1. Introduction **7**

1.1. Background 7

1.2. Problem Statement 8

1.3. Objectives: 8

1.4. Report overview: 8

2. Literature Review **9**

Overview 9

2.1. Damage modes of beams 9

2.2. Effect of crack on cantilever beams 10

2.2. Methods of determining the natural frequencies and FRFs 13

2.4. Finite Element Analysis of cracked beam 16

2.5. Learning based Anomaly detection 17

2.6. Performance measures of anomaly detection algorithms 21

Conclusion 23

3.Progress up to date **24**

3.1 Numerical investigation: 24

4. Experimental investigation **34**

4.1 Experimental setup 34

4.2 Healthy beam modal analysis 36

4.3 Cracked beam modal analysis 37

4.4 Processing vibrational data for autoencoder 38

4.5 Using healthy beam FRF data to train autoencoder. 39

4.6. Autoencoder performance evaluation 41

5. Crack progression method **42**

6.Conclusions and recommendations **44**

6.1 Recommendations 44

References **45**

List of Figures

Figure 1: (a) Difference between fracture mechanics failure and strength of materials failure (MechaniCalc, 2021) (b) Crack modes (MechaniCalc, 2021) 9
Figure 2: (a) Non-dimensional frequency vs non-dimensional crack depth of cracked beam (H.Nahvi, 2005) (b)non-dimensional frequency vs non-dimensional crack depth at varying positions..... 10
Figure 3: Procedure for detecting damage using FRF (Rupika P Bandara, 2014) 12
Figure 4: FRF example (Siemens, What is frequency response, 2020) 14
Figure 5: Coherence function of an FRF (Siemens, What is frequency response, 2020) 15
Figure 6: SVM segregating data (Ray, 2017) 18
Figure 7: (a) Dataset that is not linearly separable (Ray, 2017) and (b) Dataset which is now linearly separable with introduction of z (Ray, 2017)..... 18
Figure 8: (a) Single perceptron. (b) Schematic representation of forward feeding neural network... 19
Figure 9: Example of autoencoder structure (Tun, 2018)..... 20
Figure 10: Depiction of various prediction outcomes (Tun, 2018) 22
Figure 11: ROC curve for different outlier detection techniques (Tun, 2018)..... 22
Figure 12: Procedure for numerical investigation 24
Figure 13: Schematic of beam used in numerical and experimental investigations. 25
Figure 14:Cantilever beam FEA model..... 25
Figure 15: First 5 modes for cantilever beam 26
Figure 16: PCA autoencoder infrastructure 27
Figure 17: Principal component scores for numerical investigation 28
Figure 18: Reconstruction error for healthy beam 29
Figure 19: FEA model of Cracked beam 29
Figure 20: Node setup for cantilever beam modal analysis 30
Figure 21: Cracked beam anomaly detection visual a) node 1, b) node 2, c) node 3, d)node 4, e) node 5 31
Figure 22: Visualisation of 2-standard deviation rule anomaly detection technique 33
Figure 23: Experimental setup: a) schematic, b) picture diagram..... 35
Figure 24: Sample FRF of healthy uncracked beam..... 36
Figure 25: Damage zone of cracked beam used in experimental investigation. 37
Figure 26: FRFs for cracked and uncracked beam in experimental investigation 38
Figure 27: Sub-FRF of healthy beam 39
Figure 28: Autoencoder training procedure for experimental investigation 39
Figure 29: Principal component scores from Bandara et al (2014) 40
Figure 30: Principal component score for experimental investigation..... 40
Figure 31: Anomaly detection method flow diagram..... 41
Figure 32: Visualisation of 2-standard deviation rule for 1st sub-FRF..... 41
Figure 33: Crack progression procedure..... 43
Figure 34: Undisturbed body of size l and volume v with cut out a (P.Gudmunson, 1981) 48
Figure 35: Euler-Bernoulli beam (H.Nahvi, 2005) 50

List of Tables

Table 1: Properties of beam for numerical investigation 24
Table 2: Results of FEA simulations 26

Table 3: non-dimensionalised frequencies for cracked beams at s=0.5 30
Table 4: Number of undetected damage beams 31
Table 5: Performance evaluation parameters for numerical investigation 33
Table 6: Number of undetected damage beams using 2-standard deviation rule. 33
Table 7: FEA frequencies of healthy experimental beam 36
Table 8: Cut-off values for sub-FRFs 40
Table 9:Performance evaluation parameters for experimental investigation 41
Table 10: Average reconstruction error values for each sub-FRF 42

List of Symbols

ε_i, slack variables

l, number of data points

w, hyperplane normal vector in feature space

ρ, origin

v, bound on the fraction of outliers and lower bound on the fraction of support vectors (used to control false alarm rate)

E, Young's modulus

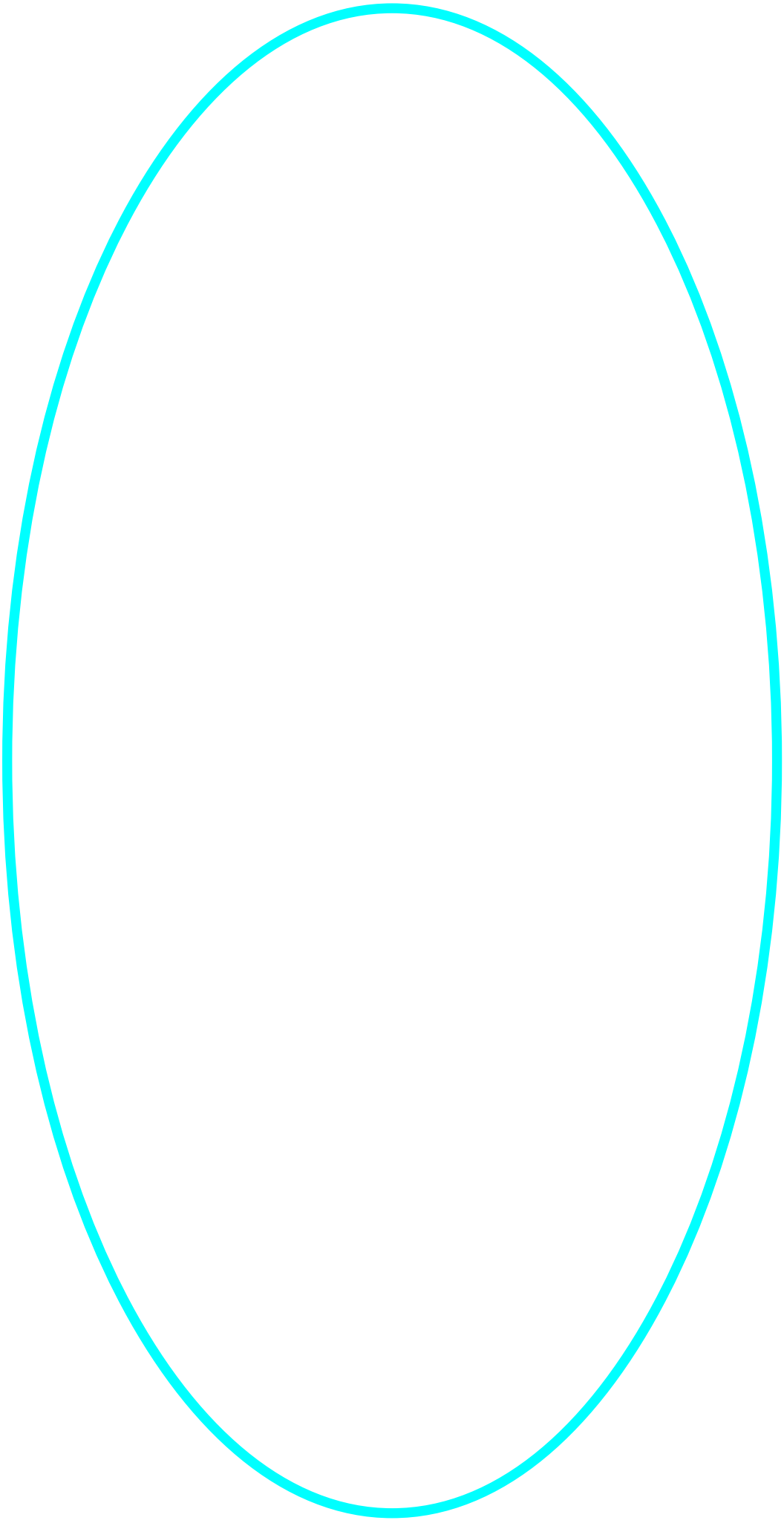

1. Introduction

1.1. Background

Structural health monitoring (SHM) are automated methods for determining changes in structural integrity of mechanical systems. SHM serves to provide assessment of a structures ability to perform its task and is therefore useful in civil, military and aerospace engineering applications (Yuan, 2016). An SHM system typically consists of diagnosis component which consists of damage detection assessment, and a prognosis component which determines consequences of the diagnosed damage. SHM is important because capital intensive assets/structures need cost-effective and reliable monitoring and inspection techniques which ensure the integrity and reliability of these structures. SHM systems can offer these solutions when combined with non-destructive testing (NDT) solutions (FCPrimeC, 2019). An example of this is seen in a study of existing structures in North America which are approaching the end of the design service life (FCPrimeC, 2019). It is reported that approximately 56000 bridges are structurally deficient and thus vulnerable to failure. Implementation of SHM systems aid in detecting the ways in which such structures are vulnerable and help maintenance engineers determine how to mitigate/eliminate vulnerabilities of existing structures. Thus, prolonging the service life of the structures. For these reasons, SHM is an important concept in engineering, which is why the development of an SHM model is investigated for this research topic. As mentioned before, SHM is efficient when coupled with NDT solutions. The NDT method utilised in this research topic is vibration-based monitoring.

Vibration based monitoring (VBM) systems allow for the observation of the global response for a structure, including damage detection, classification, and progressive development (Giosue Boscato, 2019). This is because dynamic monitoring systems have proven to be particularly suited for systems whose structural behaviours are heavily influenced by their geometric and material complexities. Also, because of its non-destructive and non-invasive nature, VBM can be safely applied to historical or damaged structures, which would potentially be dangerous under other test conditions. Therefore, the analysis of the modal behaviour can reveal structural weaknesses or deficiencies due to unforeseen phenomena such as damage as well as any progression of structural damage. Thanks to their non-invasive characteristics, VBM procedures are widely used, and several studies have addressed structural identification (especially early crack detection) through the vibration data.

As mentioned in the background, SHM plays an integral role in monitoring the integrity and reliability of a structure. SHM is best utilised when combined with other techniques such as NDT. A well-suited NDT technique to use for SHM is VBM due to its non-destructive and non-invasive characteristics. However, implementing a system of this kind can result in a large magnitude of data needing to be interpreted and processed especially if it were to be done on multiple structures (such as the 56000 bridges mentioned in the background). This means that a system of this nature would not be efficient if it were to function manually, and methods need to be implemented for such an SHM system to work in automatically assessing the structural integrity and reliability of its structures based on the data that is obtained through VBM. This creates the need for SHM methods that are data driven and can automatically process data to monitor the structural health of a system. Anomaly detection is a data driven method based on determining the outliers of a dataset and thus presents a possible solution to the need for data-driven methods in VBM. Studies such as ‘Structural damage detection method’ by Bandara et al (2014) combines VBM with anomaly detection techniques to detect damage on structure based on the frequency response of the structure. Other studies include the ‘Computer-vision and deep learning-based anomaly detection for Structural health monitoring’ by Bao et al (2018) which used neural networks to monitor unchecked SHM data

and look for damage. This highlights the potential of anomaly detection as a data driven model for SHM.

1.2. Problem Statement

Based on the idea that data driven models can be implemented in SHM and more specifically VBM. There is a potential need to develop an automatic damage detection method (structural health monitoring system) for cantilevered beam using data-driven models. The data-driven model will be an anomaly detection model which utilises machine learning to analyse the data. The idea is that the method would form part of a diagnosis component of an SHM system which is able to detect if the cantilevered beam has damage. The project has two objectives. The primary objective is to develop an algorithm that can detect damage on the beam. This method needs to work for simulated and experimental VBM data. The secondary objective is to determine if the method developed can also assess the damage in terms of the progression of damage to the cantilevered beam. The research topic is successful if the primary objective is met.

1.3. Objectives:

The objective of this research task is to develop a data driven model which serves as a form of anomaly detection for cantilevered beams. The model will use data obtained from vibrational analysis along with anomaly detection techniques. For this task anomaly detection machine learning techniques will be utilised, and the anomaly detection algorithm must utilise historically healthy/ non-anomalous data to train the anomaly detection algorithm. This model needs to work for real-world VBM data and is considered a success when it can detect damage based on real-world VBM data (this is the primary objective of the study). If this can be completed a secondary objective is then considered in which it is investigated if the model is able to monitor the progress of the crack. The model is successful if the primary object is met. The development of this model will include a numerical investigation (to determine if the anomaly detection method is useful for vibrational data analytically speaking) and an experimental investigation to investigate if the model is able to work on data obtained from experiments.

1.4. Report overview:

The report comprises of a literature review, numerical investigation, reflection on the way-ahead for the project. In the literature review, topics such as the damage modes of structures, manifestation of damage in vibrational data, methods of obtaining vibrational data, finite element analysis of vibrational data, anomaly detection and performance metrics for anomaly detection are discussed. In the numerical investigation, the concept of using anomaly detection for analytical and simulated data is analysed. In the reflection on the way ahead, an overview of the work which still needs to be completed and the projected timelines for when this work will be completed is given.

2. Literature Review

Overview

In the literature review, section 2.1 discusses the damage modes of a structure and more specifically cantilever beams are discussed. In section 2.2 the manifestation of damage in the behaviour of cantilevered beams is discussed. It is seen that the damage caused by a crack reduces the stiffness of the beam and results in changes of vibrational characteristics. Section 2.3 discusses the procedures to determine the vibrational characteristics analytically and experimentally. Section 2.4 discusses a procedure for finite element analysis of a cracked beam. With the physics of the problem now being understood, section 2.5 discusses anomaly detection and examples of where it has been used is discussed. Section 2.5 also discusses the concept of machine learning is introduced and the various machine analyzed. Section 2.6 discusses the performance metrics for anomaly detection algorithms.

2.1. Damage modes of beams

Fracture mechanics is often the methodology used to predict failure in structures due to the presence of flaws, and mainly cracks (MechaniCalc, 2021). Fracture mechanics is important because the presence of a crack magnifies the stress around the crack, resulting in a part failing earlier than what would be expected using traditional strength of material methods (i.e., when the yield or ultimate stress of a material is reached, depending on the failure criteria). In fracture mechanics, a part fails when a stress intensity factor-which is calculated using the applied stress, part geometry and crack size-exceeds the fracture toughness of the materials. Figure 1a shows the difference in failure modes using the fracture mechanics methodology compared to the strength of material methodology.

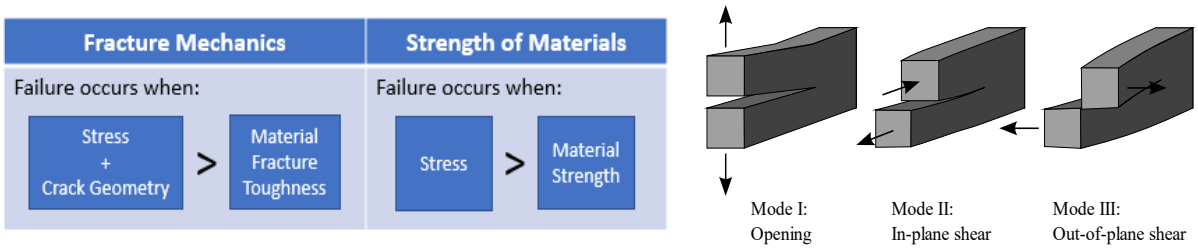

Figure 1: (a) Difference between fracture mechanics failure and strength of materials failure (MechaniCalc, 2021) (b) Crack modes (MechaniCalc, 2021)

The analysis of cracks is looked at in this report since cracks and crack like flaws occur more frequently than expected (MechaniCalc, 2021) due to pre-existence within a part or developing due to high stress/fatigue. When a load is applied to a cracked part, there are 3 primary modes of loading that the crack tends to exhibit. These modes are exhibited in figure 1b. Mode 1 is a normal opening mode, mode 2 and mode 3 are shearing modes (mode 2 being in-plane shear and mode 3 being out-of-plane shear). In engineering practice, mode 1 is most analyzed as it is the worst-case scenario, and the shearing modes will evolve into mode 1 as the crack worsens. The mode being analyzed characterizes the stress intensity factor of a structure (which in turn characterizes the stress field near the crack). In general, the stress intensity factor of a crack is given by the following equation:

$$K = Y\sigma\sqrt{\pi a} \qquad (1)$$

Where Y is the geometry factor,a is the crack size and σ is the applied stress? For an edge crack of a semi-infinite plate (which is the type of crack which is often employed in studies). The geometry factor often is equal to 1.12. The stress intensity factor is utilized in design and analysis by arguing that the material can withstand crack tip stresses up to a critical value of stress intensity, termed K_{1C}, beyond which the crack propagates rapidly (Roylance, 2001). It is for this reason that the modelling of the crack is an important factor to consider when using damage detection in beams.

2.2. Effect of crack on cantilever beams

Adams et al (1979) found that fibre-reinforced plastics have a state of damage that is detectable by a reduction in stiffness and an increase in damping. These changes in stiffness, whether local or distributed, result in decreases in the natural frequencies of a vibrating system. This means that damage of a structure can be detected by measuring the natural frequencies of a structure at two or more stages of life. Furthermore, the magnitude of the frequency changes can also be used to assess the magnitude of the damages to the structure. The study shows that the presence of damage can be detected simply from changes in the natural frequencies without the need for any analysis other than that which was done to determine the frequencies and that damage could be detected for at the very least 0.1% of area removal of a shell structure.

A study by H. Nahvi et al (2005) presents an analytical and finite element analysis method to determine the changes in the natural frequencies of a beam by studying the effect of a crack on the flexibility coefficient of the beam (which affects the vibration response under external loads) of a structure. This study also aims at being able to determine the crack location and size of a structure (namely a cantilevered beam). The new flexibility coefficient of the cracked beam (which uses both the flexibility coefficient of the uncracked beam and the crack) is then used to compute the natural frequencies and mode shapes of the cracked beam. The natural frequencies and mode shapes are calculated at a normalized distance x/l from the beams fixed position and at non-dimensionalised crack depth s. The effect of these parameters on the natural frequencies is measured using the non-dimensionalised natural frequency which the ratio of the natural frequency of the cracked beam to the natural frequency of the uncracked beam. During the analysis, the beams are divided into elements with element 1 being the closest to the fixed end of the beam and element 5 being the furthest away from the fixed end. The results are shown in figure 2a

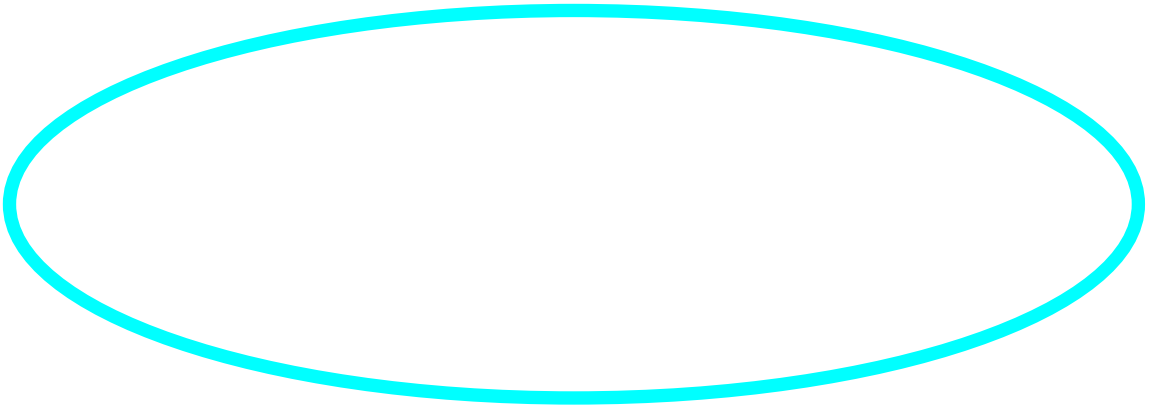

Figure 2: (a) Non-dimensional frequency vs non-dimensional crack depth of cracked beam (H.Nahvi, 2005) (b)non-dimensional frequency vs non-dimensional crack depth at varying positions

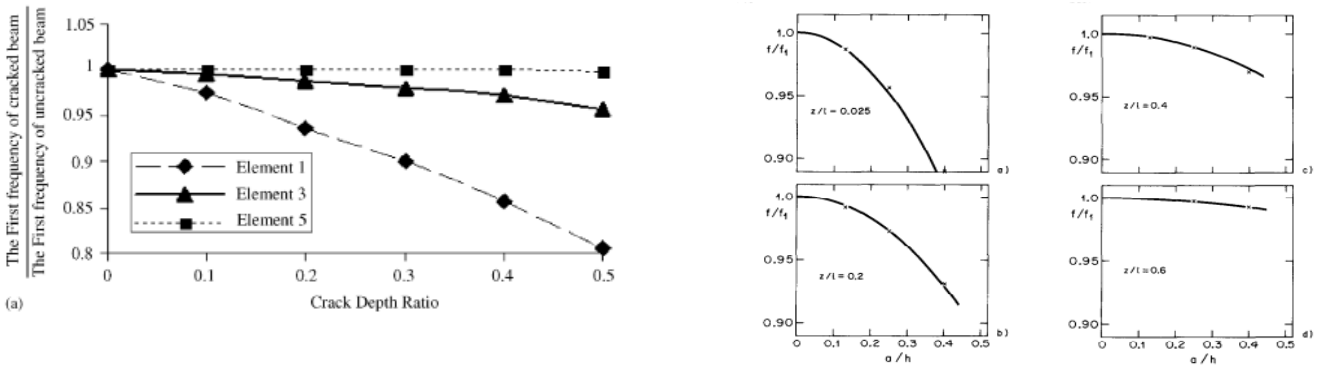

It is evident the non-dimensional frequency decreases with increasing non-dimensionalised crack depth. This agrees with the statement made by Adam et al, in terms of the belief that the presence of a crack reduces the stiffness which in turn reduces the natural frequency of the structure. Another thing that becomes evident is that the first element is affected the most by the crack whilst the 5th [t] element is affected the least by the crack, implying that the position of the crack relative the fixed end influences the deviation of the natural frequency of the structure. This is because the crack affects the stiffness of the beam near the support, as a result, the closer it is to the support the more it will affect the stiffness and thus reduce the natural frequency.

A study by P. Gudmunson (P.Gudmunson, 1981), presents a method to determine the changes in eigenfrequencies of a structure due to geometrical changes such as cracks and notches. The study presents a first order perturbation method which can predict the changes of a structure's eigenfrequency due to the strain energy changes of the structure. The technique is applicable for small cracks and other small cut outs. The technique was evaluated with cantilever beams and is shown to correlate well with numerical and experimental results. The idea behind the perturbation method is to model the damaged structure as its own system which utilizes the fundamental frequency equation (in the same way that the undamaged system does) and create a relative system to determine the change in frequency and mode behaviours of the structure between the damaged and undamaged systems. A more complete explanation of the method is presented in appendix A1.

Using this method, Figure 2b shows the graphical representation of how the natural frequency deviates for a cracked cantilever beam as the size of the crack increases. The data happens to agree with the information presented by Adams et al, which is that as the crack growth increases the natural frequency of the cantilever beam decreases. This phenomenon was also noted in the study by Nahvi et al. Another observation of the perturbation method which is consistent with the compliance method is that as the crack is moved further away from the fixation point, the rate at with the natural frequencies deviate from the uncracked specimen tend to decrease.

Another thing that is mentioned in the study is that the experimental results tend to correlate more with the analytical results when the crack is located further from fixation.

A study by Bandara et al (2014) utilizes the frequency responses functions (FRFs) of a structure to detect damage (FRFs are discussed in section 2.3). FRFs offer the dynamic behaviour of a structure over a frequency range compared to the previous methods discussed above which show how a structure should behave only at specific frequencies. This allows for FRF data to be used for damaged assessment without any intermediate steps compared to the other methods discussed which require mathematical models to extract the modal data such as the natural frequencies. The study combines the use of FRFs with Neural Networks (discussed in section 2.4). Neural networks have excellent pattern recognition, auto-association, self-organization, self-learning, and nonlinear modeling capability. Also, neural networks can extract precise and reliable information from

imprecise, unreliable, inconsistent, uncertain, and noise-polluted data, making them useful for analyzing data within FRFs. The type of neural network used is principal component analysis (PCA) and it is used to reduce the size of the FRF data and filter out unwanted noise. According to Bandara et al (2014), many studies which have employed this method struggle to accurately detect light damage to a structure. For this reason, the study proposed a method of dividing up the FRF data from the experiments in the following way (complete derivation is available in ref [(Rupika P Bandara, 2014)] (Figure 3 displays the used procedure.):

- The FRF data is used in matrix $[H]_{dam} = [h(\omega)]_{dam}$ which has m rows of data (where m is the number of sensors used in vibrational measurements) each with n number of frequency points. The same is done for an undamaged structure.
- The dataset is then divided into subsets with r number of frequency points (where r<n)
- The data subsets processed to be used in the PCA algorithm. When a PCA algorithm is used it determines components/features that are orthogonal to each other within the data. The principal components are the components with the highest eigenvalues and the associated eigenvector, and they represent the direction and amount of highest variability (i.e., the algorithm determines which features will have the highest amounts of variability and this can help determine which features should be used to detect damage). This helps in reducing noise because the components with low eigenvalue scores can be discarded. Using these PCs, reconstructed FRF matrices are created for the damaged and undamaged structures. A damage index (DI) is created which is essentially the ratio of the damaged FRF matrix to the undamaged FRF matrix. The reason for introducing DI values is that changes in the shape of the FRFs due to structural change cause the DI to change. Changes in the shape of the FRF can include peak frequency change, peak amplitude change, and FRF slope change. These changes correspond to natural frequency, mode shape, and damping ratio, respectively. Modal parameters which are

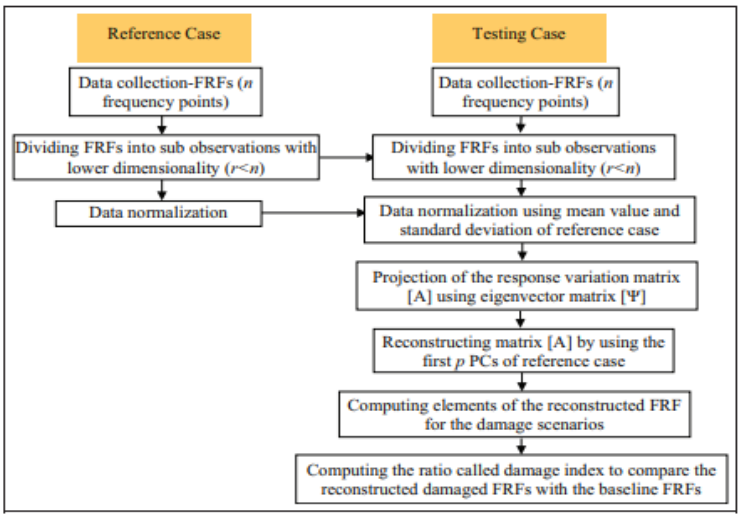

Figure 3: Procedure for detecting damage using FRF (Rupika P Bandara, 2014)

  often used in damage detection and location.

FRF data was then conducted on a 3-story bookshelf, and it was seen that there was a 1.75 % percent error in detecting damage and a 1.98% error in estimating the severity of the damage. It is important to note that the performance metric used in this study is the mean-squared error, which is not one of the performance metrics that are normally used for anomaly detection (these metrics

are discussed in section 2.5). However, this study shows the usefulness of FRFs and neural networks in detecting damage of a beam.

2.2. Methods of determining the natural frequencies and FRFs

From the studies analyzed in section 2.2 it is evident that 2 successful ways of detecting damage in a structure are by determining the natural frequencies or by utilizing an FRF. This section of the literature review aims on providing information as to how the natural frequencies of a cantilevered beam are determined analytically and experimentally.

To analytically find the natural frequencies of a structure, it is regarded as a multiple degree of freedom (MDOF) vibrating structure and the following equation is used (Yung-Lee, 2012):

$$m\{\ddot{x}\} + C\{\dot{x}\} + k\{x\} = F(t) \quad \textbf{(2)}$$

Where m represents the mass matrix of the structure, C represents the damping matrix, k represents the stiffness matrix, x is the displacement response vector of the structure and F(t) is the force vector as a function of time.

The natural frequencies are evaluated at free vibration conditions, where $C\{\dot{x}\}$ and $F(t)$ are equal to zero, meaning equation 2 is reduced to the following equation:

$$m\{\ddot{x}\} + k\{x\} = 0 \quad \textbf{(3)}$$

This can be viewed as a differential equation with the solution being:

$$\{x\} = \{a\}\sin(\omega_n t - \alpha) \quad (4)$$

Where $\{a\}$ denotes the vibration modes and ω_n is the natural frequencies of the modes. Substituting equation 4 into equation 3 and completing the necessary mathematical tasks, equation 3 is converted to the following equation:

$$[[K] - \omega_n{}^2[M]]\{a\} = 0 \quad \textbf{(5)}$$

Because the natural modes ({a}) are considered not to be zero everywhere, the important equation to analytically determine the natural frequencies is given as:

$$|[K] - \omega n2[M]| = 0 \quad \textbf{(6)}$$

This is then solved by solving the determinant of the equation above. The natural frequencies can be determined as eigenvalues and the modes are determined as the eigenvectors corresponding to the eigenvalue. Therefore, the mode shapes are either real or complex and have a natural frequency assigned to each mode.

Analytically the natural frequencies of a beam can be calculated using the following equation (Autofem, 2021):

$$f_i = \frac{1}{2\pi}\sqrt{\frac{EI}{\rho S}}\left(\frac{k_i}{l}\right)^2 \quad \textbf{(7)}$$

Where f_i is the ith natural frequency and k_i is a factor that depends on the mode of vibration ($k_1 = 1.875, k_2 = 4.694\ and\ k_3 = 7.855$). Calculating the natural frequencies experimentally requires an understanding what happens at the natural frequency.

When a structure is excited at its natural frequencies, a phenomenon known as resonance occurs. This is characterized by the dynamic force exciting the structure producing a large vibration response (Siemens, Natural frequency and resonance, 2019). Therefore, by measuring the vibration response of a system as a function of its frequencies, the natural frequencies of a system can be identified by

analyzing the peak responses of the system and this is often done through utilizing FRFs. Using this technique these natural frequencies are often referred to as resonant frequencies.

An example of an FRF is given in figure 4. FRFs are time-invariant transfer functions that express the relationship between an input function and output function in the frequency domain (Siemens,

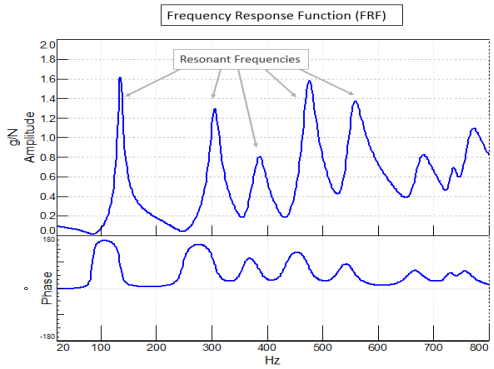

Figure 4: FRF example (Siemens, What is frequency response, 2020)

What is frequency response, 2020).

FRFs display the amplitude (which is usually the magnitude of the structure's vibration response) as a function of the frequency which the structure has been is being excited at. The natural frequency is then identified through resonance (i.e., large spikes in amplitude in the FRFs). FRFs can be generated with various inputs and outputs for example:

- Mechanical systems often take the force (in newtons) as an input and the output is usually the acceleration (in g's) or the displacement function (in metres)
- Acoustic systems take the volume acceleration, and the output is the sound pressure
- Rotating mechanical systems take the torque (Newton-metres) as an input and the output is the rotational displacement (degrees or radians)

For mechanical systems, the transfer function is usually described by the following equation:

$$[\mathrm{H}(\mathrm{j}\omega)] = \frac{\{\mathrm{X}(\mathrm{j}\omega)\}}{\{\mathrm{F}(\mathrm{j}\omega)\}} \quad \textbf{(8)}$$

Where X and F are the displacement (or sometimes acceleration), and force functions and H is the transfer function which is the FRF. Because FRFs have amplitudes and a phase (which describes how the output moves relative to the output and is expressed in degrees), it is a complex function containing real and imaginary components. Analyzing the imaginary components lead to the following relationships:

$$Amplitude = \sqrt{imag^2 + real^2}$$

$$phase = tan^{-1}\left(\frac{imag}{real}\right) \quad \textbf{(9)}$$

At resonance two events occur: firstly, the real component of the amplitude is zero and the FRFs will generate "peaks" above or below zero and this can be used to determine the mode shape of a structure. One more concept of an FRF that needs to be understood is that of coherence.

Figure 5 gives an example of a coherence graph. Coherence is function versus frequency that indicates how much of the output is due to the input in the FRF (Siemens, What is frequency response, 2020). It can be indicator of the quality of the FRF and evaluates the consistency of the FRF to repeat the same measurement when the system is excited again.

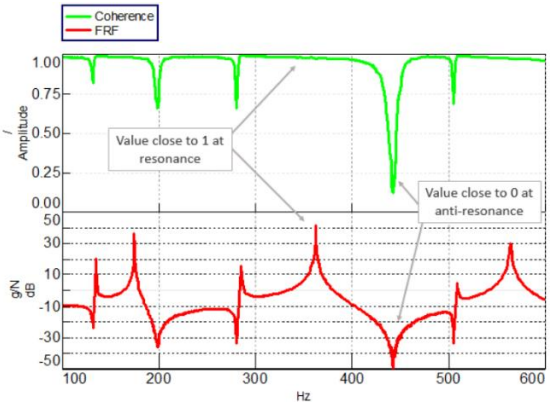

Figure 5: Coherence function of an FRF (Siemens, What is frequency response, 2020)

Coherence ranges from 0 to 1, with 1 being very repeatable (i.e., consistent) and 0 being not repeatable (thus inconsistent which and indicative of measurement error). A trend of FRFs is that it should have high coherence at resonant frequencies and low coherence at anti-resonance (due to inconsistencies generated from the noise floor of the instruments used). In general, if coherence is closer to 0 than to 1 at resonant frequencies or across the frequency range than there is a problem with the measured FRF. With a comprehensive explanation of FRFs being given, how FRFs are recorded is discussed next. When doing vibration analysis of machines there are usually 2 types of methods that can be tested (Rao):

- Operational deflection-shape measurement:
  Measures the vibration response (dynamic system shape) of a system under steady state operating frequency. This method is only valid for forces or frequencies at the specified operating conditions and thus will not yield the desired data for the objectives of the research task.
- Modal testing (i.e., modal analysis)
  This involves analysis of the modes, mode shapes, modal frequencies and modal damping ratios of a structure resulting in the complete dynamic description of the structure. Because of this modal analysis is the preferred measurement technique and will be looked at in further detail.
  Modal analysis requires the following hardware (Rao):
    a. Exciter: Vibration source to apply input force to structure. The types of exciters of used are electrical shakers and modal hammers. Electromagnetic shakers provide large input forces so that the response is measured easily. The force is a large harmonic input of magnitude F applied at discrete frequencies within a frequency range of interest. At each frequency, the structure must first be in steady state before the magnitude and phases are recorded. The other type of exciter which can be utilized is a modal hammer which is a hammer with a built-in transducer (to measure the force of impact) that impacts/hits the structure. The response of the structure or machine to an impulse (created from the impact) is composed of excitations at each of the natural frequencies of the structure. Shakers have advantage of being able to produce large forces in the correct direction for accurate results, whereas modal hammers have the problem of sometimes not being able to produce large enough excitations to produce sufficient

response signals. However, modal hammers do have the advantages of being easier to set up and do not have significant mass loading effects like the shaker does.

b. Transducer: Converts physical output response into electrical signal. The two types of transducers that are analyzed are accelerometers and vibrometers. Accelerometers are the most used transducer. Accelerometers measure the acceleration response of a structure over time. The issue of an accelerometer is that the accelerometer has its own natural frequency, and the maximum measurable frequency of the accelerometer is a fraction of its own natural frequency. This will affect how precise the recorded natural frequencies are. Another issue is that their weight can create slight mass loading effects which can affect the expected behaviour of the structure. They are however preferable with regards to experimental setup as they just need to be attached to the structure and connected to the signal conditioning amplifier. Laser Doppler vibrometers (LDVs) measures the displacement of a vibrating body by using laser light reflected by the moving surface of the structure (Francesco Trainotti, 2020). The biggest advantage of using LDVs is that they reduce the effect of mass loading effects since light is used to measure the vibration response. They are, however, more difficult to set up experimentally.
c. A signal conditioning amplifier allowing transducer to be compatible with data acquisition system
d. An analyzer to perform signal processing and modal analysis with a suitable software

2.4. Finite Element Analysis of cracked beam

A proposed method by Meshram et al (Nitesh A. Meshram, 2015) uses the fact the stiffness is reduced by the presence of a crack and that a new stiffness matrix needs to be calculated for a cracked beam element using the following equation:

$$[Kc] = [K]_{uncracked} - [K]_c \quad \textbf{(10)}$$

Where $[Kc]$is the stiffness matrix of the cracked cantilever beam, $[K]_{uncracked}$ is the stiffness matrix of the uncracked cantilever beam element and $[K]_c$ is the reduction in stiffness of the beam due to the crack. $[Kc]$can then be substituted into equation 10 and 11 to compute the natural frequencies and modes for the cracked beam. When doing this it is important to note that the mass matrix [M] for the cracked beam is assumed to be the same as that of an uncracked beam. The issue with this method is that $[K]_c$ is usually unknown and needs to be calculated first before the cracked beam stiffness can be calculated. This can be optimized by using the model described by H. Nahvi et al in which the stiffness matrix for a cracked model has already been derived based on the flexibility of the element. This cracked stiffness element can be described the following equation:

$$[K_C] = \frac{1}{C_{11}C_{22} - C_{12}C_{21}} \times \begin{bmatrix} C_{22} & C_{22}l - C_{21} & -C_{22} & C_{21} \\ C_{22}l - C_{21} & C_{22}l^2 - C_{21}l - C_{12}l + C_{11} & -C_{22}l + C_{12} & C_{21}l - C_{11} \\ -C_{22} & -C_{22}l + C_{21} & C_{22} & -C_{21} \\ C_{12} & C_{12}l - C_{11} & -C_{12} & C_{11} \end{bmatrix}. \quad \textbf{(11)}$$

The equations used to obtain the flexibility coefficients are available in ref (H.Nahvi, 2005). When the FEA procedure is carried out and the non-dimensional natural frequencies of the beam are determined. The expected trend (i.e., that the natural frequency decreases with increasing crack

size, which is discussed in section 2.2) is seen. When compared to experimental results in the study it is seen the FEA solution has a 0.4% error in computing the crack location and a 1.2 % error for computing the crack size for the first frequency mode and a 0.3 % error in computing crack location and a 10% error for computing crack size in for the second frequency mode.

2.5. Learning based Anomaly detection

Anomaly detection/ outlier analysis is a technique that identifies data points, events, and/or observations that deviate from a dataset's normal behavior (i.e., an anomaly). Anomalous data can indicate critical incidents, such as errors in a structure or indicate new phenomenon that allows for potential growth of a field (Cohen, 2021). Anomaly detection is commonly used in areas such as: Data cleaning, intrusion detection, fraud detections, system health monitoring, event detection and ecosystem disturbances (Johnson, 2021).

Examples of how anomaly detection have been used in engineering fields include the study of Bandara et al (Rupika P Bandara, 2014) discussed in section 2.3. Y. Bao et al (Yuequan Bao, 2018) developed an anomaly detection method to detect potential anomalies in large amounts of unchecked structural health monitoring data using computer vision and deep neural networks. The results yielded an 87% accuracy of a 1-year test dataset and is believed to be suitable proposed method to SHM. Also, a study by Konstantinos et al (Trichias Konstantinos, 2014) present a procedure for local structural health monitoring by applying Anomaly Detection (AD) on strain sensor data for sensors that are applied in expected crack path. Sensor data is analyzed by automatic anomaly detection to find crack activity at an early stage. These studies show the usefulness of anomaly detection in SHM systems.

Generally speaking, there are 3 main categories of anomalies:

- **Global outliers**: Point anomalies where the outliers exist far outside the entirety of the dataset (i.e., the point is an anomaly in every metric).
- **Contextual outliers**: Conditional anomalies in which the outlier has data points which deviate significantly from other data points that exist in the same context.
- **Collective outliers**: When a subset of data points within a set is anomalous to the entire dataset, those values are called collective outliers. Individual values are not anomalous globally or contextually. These types of outliers become evident when examining distinct time series together. Individual behavior may not deviate from the normal range in a specific time series dataset. But when combined with another time series dataset, more significant anomalies become clear.

Anomaly detection does come with challenges (Johnson, 2021). Building an anomaly detection is tedious to do by hand as it requires a large amount of knowledge in the domain of the system and foresight. If you are working with systems where the data changes over time, this becomes a problem as the system will then consistently need to be revisited and manually corrected. This results in the system being time-consuming to maintain (i.e., it becomes time-consuming to make sure that the system can adapt). This is something can be overcome using machine learning.

Machine learning is a data analytics technique which is a subset of artificial intelligence (AI) that provides systems the ability to automatically learn and improve from experience without being explicitly programmed. Machine learning focuses on the development of computer algorithms that can access data and use it to learn automatically (a.i, 2020). Machine learning is well suited to anomaly detection because it works better due to having faster computational time, is adaptive and can handle larger datasets.

When utilizing machine learning algorithms, it is important to make sure that the selected algorithm is well suited to the task it has been chosen for. In anomaly detection, the types of algorithms which are used fall into 3 different categories depending on how the dataset is supposed to look like (Tun, 2018). These are:

- Unsupervised detection algorithm: This type of algorithm is utilized for datasets that have no labels (in terms of the data being labelled as normal or outlier). The algorithm assumes that majority of the dataset is normal and the data that is different is considered to be an outlier. The algorithm does not require training data and only needs the testing dataset.
- Supervised detection algorithm: Algorithm is utilized for datasets that are labeled (i.e., 'normal data point' and 'outlier data point'). It essentially detects anomalies through classification.
- Semi-supervised detection algorithm: The dataset is labeled. However, the training data is only comprised of normal data. An unsupervised algorithm is trained using the training data. Then the algorithm is tested using data which contains outliers. This algorithm uses the logic that outliers are observations that deviate from normal data.

The idea behind the research topic is that the automatic damage detection system is trained with only healthy beam data. This would imply that the most suitable algorithm to choose is a semi-supervised detection algorithm. This means that the type of machine learning algorithms that will be analyzed in this literature review will be algorithms best suited to semi-supervised detection. The first algorithm to be discussed is support vector machines (SVMs).

SVMs are classification-based machine learning algorithms that plot each data item as a point in n-dimensional space where n is the number of features in the dataset (and the value of each feature being the value of a particular coordinate) (Ray, 2017). Classification is then performed by finding a linear hyper-plane that differentiates the two classes (normal or anomaly) very well. The support vector is the co-ordinates of each individual observation, and the hyperplane is used to segregate

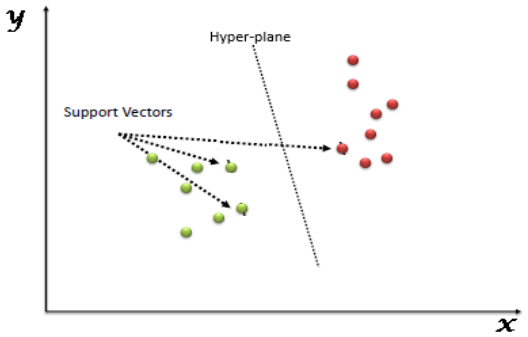

Figure 6: SVM segregating data (Ray, 2017)

the two classes. An example of how the SVM works is shown in figure 6

The distance between the nearest data point and the hyperplane is known as the margin and a greater margin leads to greater robustness as well as reduced risk of misclassification. The two classes may not always be linearly separable on x and y as shown in figure 7 (a).

Figure 7: (a) Dataset that is not linearly separable (Ray, 2017) and (b) Dataset which is now linearly separable with introduction of z (Ray, 2017)

For a linear hyperplane to segregate the two classes, SVM utilizes a kernel trick which takes the low-dimensional space and transforms it into higher dimensional spaces to find a hyperplane that best segregates the two classes. So, for an example like this, the kernel may introduce a feature z=x^2+y^2. If z is now plotted against x (seen in figure 7b). A linear hyperplane can now be used to separate normal data from outlier data. This is helpful for non-linear data and is what makes the SVM useful in anomaly detection techniques. One of the SVMs that is considered for semi-supervised detection algorithms is the one-class SVM, which separates outliers from the origin with maximum margin (Tun, 2018). The observations inside the separating boundary (hyperplane) are predicted as normal observations ($\widehat{y_i} = 1$) and the observations outside the boundary are predicted as outliers ($\widehat{y_i} = -1$). One class SVMs can be optimised by minimising objective function:

$$\frac{1}{2}\|w\|^2 + \frac{1}{vl}\sum_{i}^{l}\varepsilon_i - \rho \quad \textbf{(12)}$$

Having to meet the following constraints:

$$y_i(w.x_i) \geq \rho - \varepsilon_i \; for \; i = 1,2,\dots n \quad \textbf{(13)}$$

$$\varepsilon_i \geq 0 \; for \; i = 1,2,\dots n$$

The one-class SVM can utilize the gaussian kernel which follows the equation:

$$K(X,Y) = e^{-\frac{|X-Y|^2}{2\sigma^2}} \quad \textbf{(14)}$$

Before the next model is described it is important to explain the concept of neural networks. The field of neural networks are often referred to as Multilayer Perceptrons (Brownlee, Crash course on multilayer perceptron neural network, 2016). A perceptron is single neuron within a network intended to be a linear classifier which classifies input by separating two categories with a straight line (Leonel, 2018). The input is often described by a feature vector x multiplied by weights w and is added to bias b (the bias is the flexibility of the neuron, in terms of being able to move the predicted function up or down to better fit the model being used). This is given by the following equation:

$$y = wx + b \quad \textbf{(15)}$$

Where y is the output of the single perceptron for a linear activation function. Perceptrons produce an output based on multiple real-valued inputs, done by utilising a linear combination of input weights and subjecting the output to an activation function. This is seen in the equation below:

$$y = \varphi\left(\sum_{i=1}^{n} w_i x_i + b\right) = \varphi(W^T x + b) \quad \textbf{(16)}$$

Where W is the weight vector and φ is the activation function of the regression model being utilised. An example of a single perceptron is shown in figure 8a.

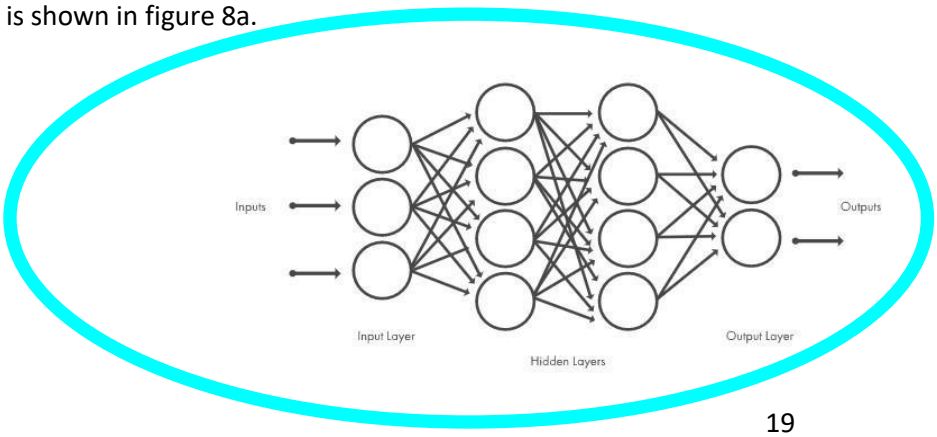

Figure 8: (a) Single perceptron. (b) Schematic representation of forward feeding neural

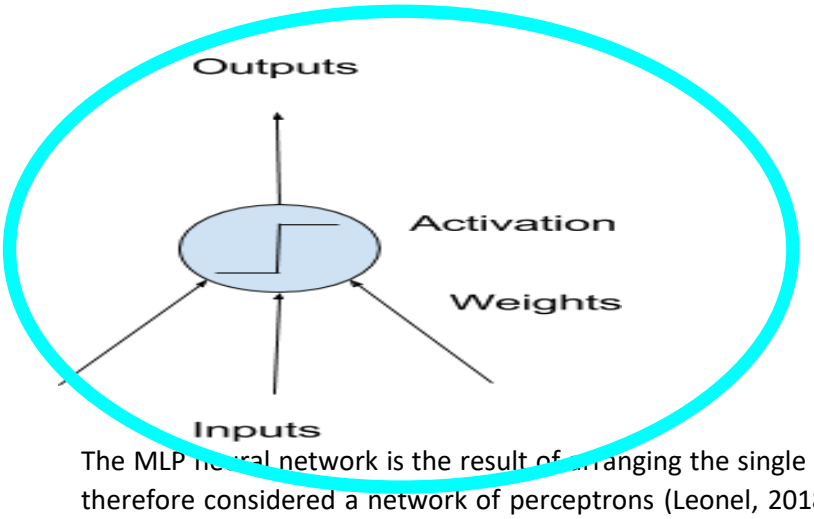

The MLP neural network is the result of arranging the single perceptrons into different layers and is therefore considered a network of perceptrons (Leonel, 2018). The layers of an MLP are separated into two different types, which are visible layers and hidden layers. The visible layers are the layer where the inputs are taken, and outputs are returned. Often a neural network is drawn with a visible layer with one neuron per input feature in your dataset. These are not neurons as described above, but simply pass the input value through to the next layer. Hidden layers are all the MLP layers not directly exposed to the input. The most simplistic neural network will always have at least 1 hidden layer (where the output layer is). More hidden layers in neural network results in a better performance. However, the cost of this is computing time. However, this problem can be overcome by using online tools that speed up this process dramatically.
In an MLP the final layer is always the output layer. The output layer is responsible for always returning an output value or an output vector of values. A schematic of an MLP neural network is shown in figure 8b. The next algorithm which is discussed utilizes multilayer perceptrons/neural networks and it is known as an autoencoder.

An example of an autoencoder structure is shown in figure 9. Autoencoders are neural networks in which the input and output variables are the same (Tun, 2018). The autoencoder essentially deconstructs the input data and attempts to reconstruct it. An autoencoder comprises of an encoder and a decoder. The encoder takes the input data and reduces the dimensions of it. The decoder then takes the data from the encoder and attempts to construct output data that is identical to the input data.

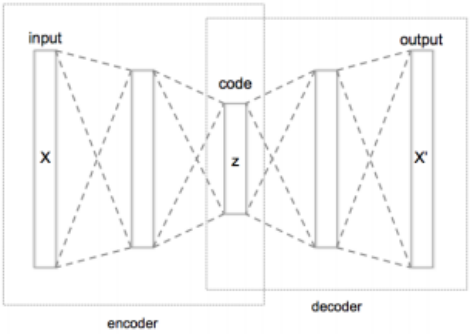

Figure 9: Example of autoencoder structure (Tun, 2018)

An autoencoder is useful for semi-supervised anomaly detection because by training the neural network with normal data, outliers can be detected by the errors during the reconstruction of the input data. When developing and training an autoencoder the following hyperparameters are considered (Dertat, 2017):

- Number of nodes in middle layer (i.e., the code). A large number of nodes results in less compression (dimensional reduction) while a smaller amount of nodes results in more compression
- Number of layers of hidden layers: Can be as deep as desired, however, the number of hidden layers in the encoder must be identical to the number of hidden layers in the decoder
- Number of nodes per layer. Which plays role in performance of each layer and the way in which the data is compressed (the number of nodes per layer usually decreases in the encoder and increases in the decoder as their structures are identical).
- The loss function: Mean-squared error (MSE) or binary cross entropy are typically utilized for autoencoders.

The chosen algorithm will need to be fitted to the data and its ability to predict the data would need to be evaluated. This involves the use of training, validation, and test datasets.

The training dataset is the dataset that is used to fit/train the algorithm. The machine learning algorithm learns from this data (Shah, 2017). The validation dataset is used to give an unbiased evaluation of the algorithm, but this is for frequent evaluation. This dataset is used to fine-tune the algorithm hyperparameters. The algorithm essentially sees the data but never learns from it. Instead, higher level parameters of the model are updated based on the evaluations. The test dataset is used to evaluate the model once it has been completely trained, this dataset contains data that varies over all the types of scenarios that the algorithm is expected to function in (In the case of the semi-supervised algorithm to be used in this study, the test dataset would include anomalies). For an algorithm to be successful it is imperative that the datasets used on the algorithm are split correctly into training, validation, and test data. An increasingly popular method to use is cross validation. How this method works is:

- The dataset is split into training and test data and the test data is put aside
- The training data is then shuffled and split into k groups
    - For a unique group, take it as validation dataset
    - The remaining groups as the training dataset
    - Fit the model to the training set and evaluate the model on the validation dataset
    - Keep the evaluation score and discard the model

This process is done iteratively until every sample in the training dataset was used to train and validate the dataset at least once. The advantage of this is that it helps in avoiding overfitting

2.6. Performance measures of anomaly detection algorithms

For an anomaly detection algorithm, accuracy is not a reliable way to evaluate its performance. This is because of the consequences of a false negative (i.e., the algorithm not being able to correctly detect an anomaly). For example, if a beam specimen which has a crack is deemed by the algorithm to not have a crack, the beam is more likely to fail when used for specific tasks since it is faulty. This can have expensive financial and social implications. Therefore, a different metric must be used for measuring the performance of an anomaly detection algorithm.

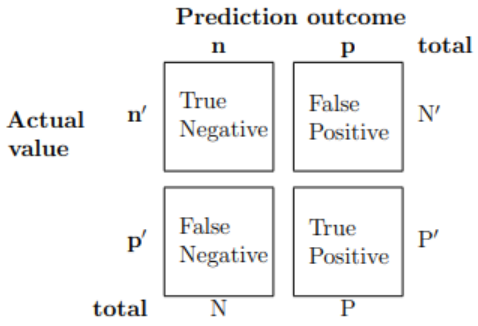

Figure 10: Depiction of various prediction outcomes (Tun, 2018)

Figure 10 shows the different types of prediction outcomes are displayed. The precision score P, the recall score R, and the false positive rate FPR are given by:

$$\begin{aligned} \boldsymbol{P} &= \mathbf{Pr}(\boldsymbol{truely\ positive}|\boldsymbol{predicted\ positive}) = \frac{\boldsymbol{TP}}{\boldsymbol{TP+FP}} \\ \boldsymbol{R} &= \mathbf{Pr}(\boldsymbol{predicted\ positive}|\boldsymbol{Truely\ positive}) = \frac{\boldsymbol{TP}}{\boldsymbol{TP+FN}} \\ \boldsymbol{FPR} &= \mathbf{Pr}(\boldsymbol{predicted\ positive}|\boldsymbol{truely\ negative}) = \frac{\boldsymbol{FP}}{\boldsymbol{TN+FP}} \end{aligned} \quad \textbf{(17)}$$

These parameters are used in two of the measuring techniques discussed in the literature review. The first technique is the area under curve (AUC) technique which is a trade-off between the true positive rate (TPR) and the FPR. This technique utilizes a receiver operating characteristic curve (ROC) which is a graph of TPR vs FPR (developers, n.d.). The ROC curve is a plot of the classification thresholds, therefore if the ROC curve plot is steep then it predicts more truly positive results and less false positive results. As shown in figure 11.

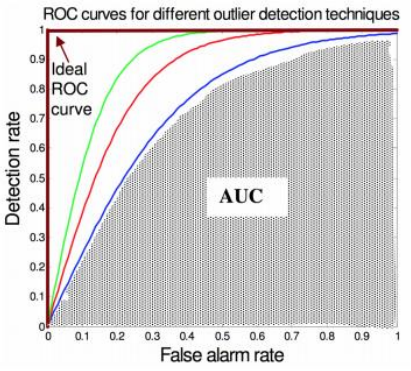

Figure 11: ROC curve for different outlier detection techniques (Tun, 2018)

AUC measures the entire two-dimensional area underneath the entire ROC curve. AUC provides an aggregate measure of performance across all possible classification thresholds. A way of interpreting AUC is the probability that the model ranks a random positive example more highly than a random negative example. In this technique TPR is equal to R and the AUC formula is given by:

$$\boldsymbol{AUC} = \int_{\boldsymbol{0}}^{\boldsymbol{1}} \boldsymbol{TPR}(\boldsymbol{FPR})\boldsymbol{d}(\boldsymbol{FPR}) \quad \textbf{(18)}$$

AUC scores range from 0 to 1, with one meaning that the model's predictions are 100% correct and 0 meaning that the model's prediction are 100% incorrect.

The AUC method has the following advantages:

- It is scale-invariant. It measures how well predictions are ranked.
- AUC is classification-threshold-invariant. It measures the quality of the model's predictions irrespective of what classification threshold is chosen.

However, the drawback of the technique is that it is not well suited to optimization (i.e., if we need to make sure that false negatives are prioritized more than true negatives)

The other technique used to measure the performance of a detection algorithm is the F-measure technique. Recall the precision score P is a measure of how well the algorithm managed to correctly detect positive results and the recall score R gives an indication of the positive results that were missed. The F-measure technique combines these two scores when both these parameters need to be considered for the performance of an algorithm (Brownlee, How to Calculate Precision, Recall, and F-Measure for Imbalanced Classification, 2020). The F-measure technique uses the following equation (Tun, 2018):

$$\boldsymbol{F-measure(F_\beta)} = \frac{\boldsymbol{(1+\beta^2)R \cdot P}}{\boldsymbol{\beta^2 \cdot P + R}} \qquad \textbf{(19)}$$

Where β is a measure of how important recall is for the model. Like AUC, the F-measure score ranks from 0 to 1, with 0 being poorest performance and 1 being 100% correct performance.

Conclusion

From the literature, the following has become evident:

- A damaged beam has a reduction in stiffness that results in a reduction in natural frequencies of a structure. This reduction in stiffness also plays a role in changing the vibrational characteristics of a structure and can therefore manifest itself in the FRF of a structure. This makes these to parameters the most ideal for detecting damage in a structure.
- The analytical calculation of the natural frequencies for a cantilevered beam can simply be given by equation 7 so long as the material and geometric properties are known and can be used to validate simulation data. Experimentally, a modal analysis experiment would be ideal for obtaining the desired parameters based on literature (i.e., the natural frequencies and FRFs). These experiments utilize an exciter, transducer, signal amplifier and analyzer. FEA of cracked beams show the expected outcome (that is that the natural frequencies decrease as the natural frequencies increase).
- Anomaly detection is a method that has been used frequently in SHM. An example of this is the one conducted by Bandara et al (2014) which is very similar in purpose to this research topic. This shows that anomaly detection is useful in SHM problems such as the one which needs to be solved for this task.
- Semi-supervised machine learning techniques are best suited for the proposed method as they train the machine learning algorithm on only normal data which is what is intended for the proposed method. Cross validation is a suitable technique that can be used to correctly train the model whilst having it be less vulnerable to overfitting.
- Performance measurement techniques best suited to anomaly detection techniques include the AUC technique and F-measure technique, however in the studies analyzed, it seems that the MSE technique was employed.

3.Progress up to date

3.1 Numerical investigation:

The purpose of the numerical investigation was to explore if a semi-supervised machine learning algorithm can determine if a cantilevered beam has damage using theoretical/ simulated vibrational data. The investigation is comprised of the following steps:

1. Generating vibrational data of a healthy beam using FEA and comparing it to analytical results
2. Using healthy beam data to create training data to train semi-supervised machine learning algorithm.
3. Generating vibrational data of damaged beams and creating test data for semi-supervised machine learning algorithm
4. Evaluating algorithm's ability to correctly detect anomalies.

The vibrational data which will be analysed for the numerical investigation is the natural frequencies. The natural frequencies are chosen to be investigated because they are directly influenced by the presence of damage and can be easily determined by FEA and analytical methods (For healthy beams). This also gives insight as to how detectable damage is when using the fact that damage influences a structures inherent behaviour (i.e., the natural frequencies).

Figure 12 shows how the numerical investigation is meant to work.

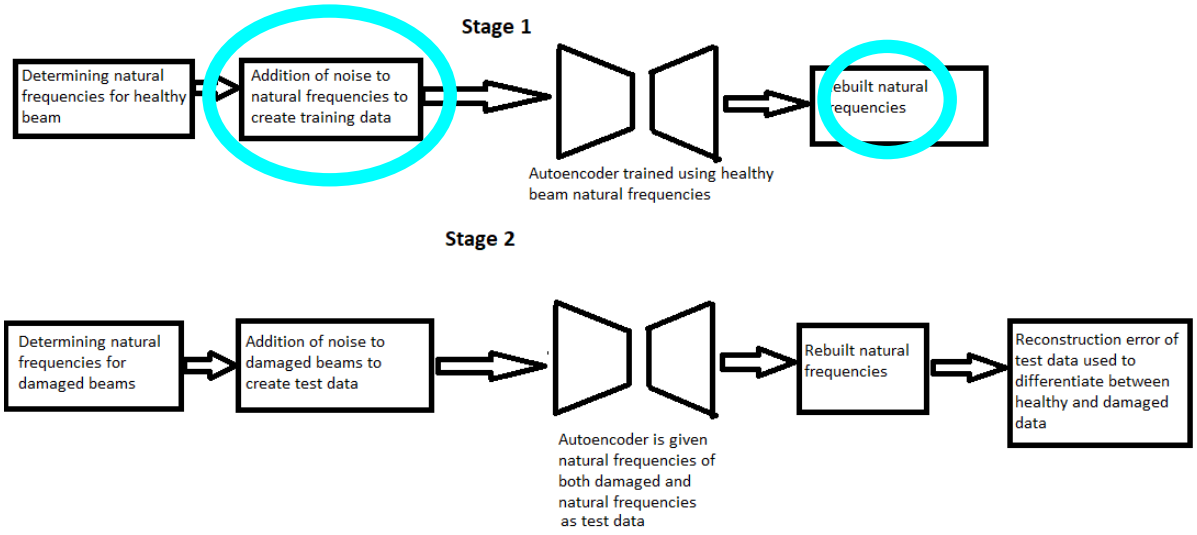

Figure 12: Procedure for numerical investigation

Following stage 2 shown in figure 12 the model's performance is evaluated.

3.1.1 Generating vibrational data.

The investigation is for a cantilevered beam with the specifications presented in table 1.

Table 1: Properties of beam for numerical investigation

Elastic modulus	175 GPa
Poisson's ratio	0.3
Density	7800 kg/m^3
Length (L)	290mm
Width (W)	13mm

Thickness (T)	22.5mm

A schematic of the beam is shown in figure 13.

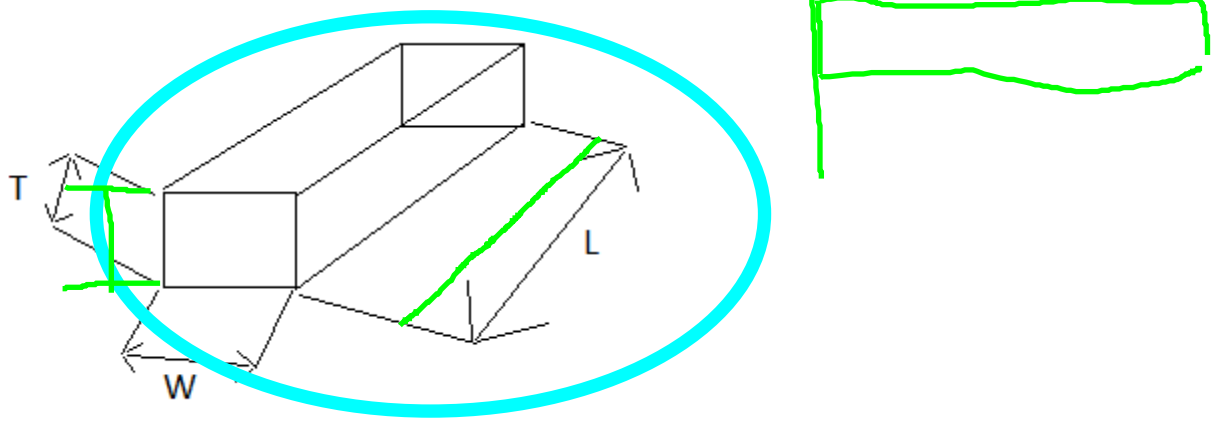

Figure 13: Schematic of beam used in numerical and experimental investigations.

This beam was selected randomly from beams which were investigated in the reports which were discussed in the literature review. This beam is from the study presented by Jabbari et al. The beam is created on ANSYS and a modal FEA is conducted. The beam is modelled to be cantilevered by adding a fixed support to one side of the beam. This is shown in figure 14. The natural frequencies for the first five modes are then generated (As seen in figure 15).

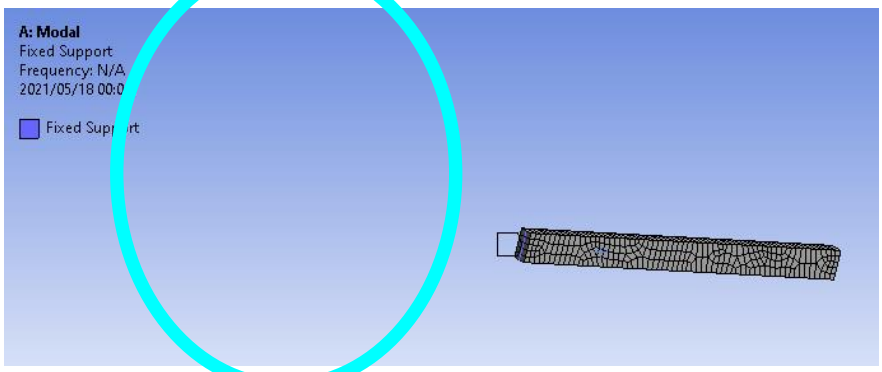

Figure 14:Cantilever beam FEA model

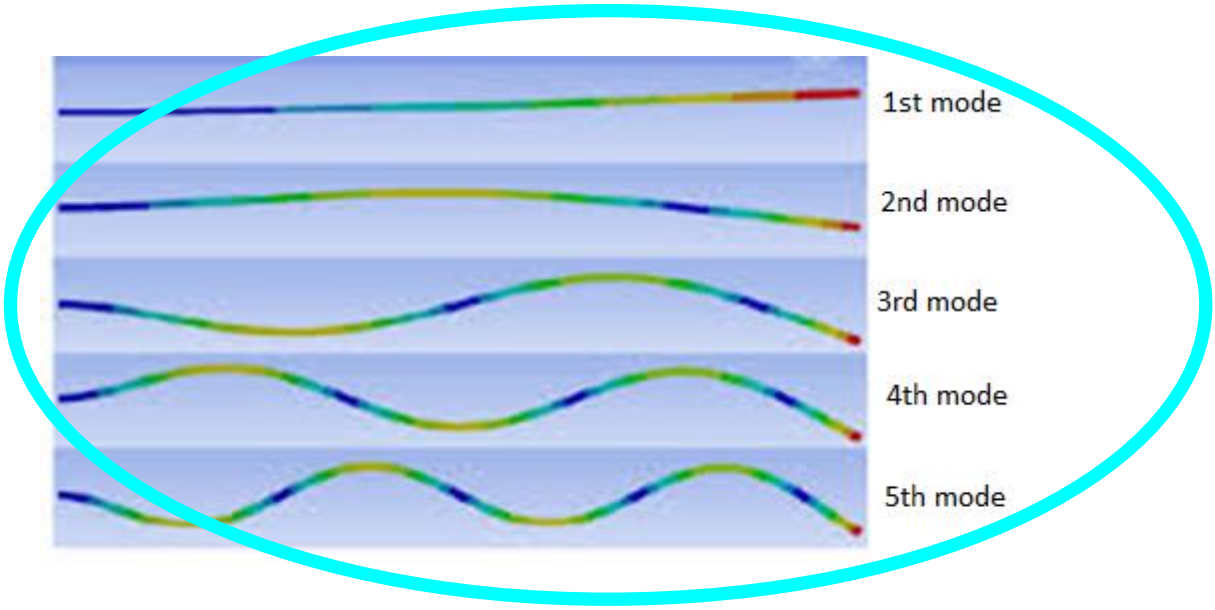

Figure 15: First 5 modes for cantilever beam

The results are seen in table 2. For validation purposes, the results of the simulation are compared to the results which would have been obtained if equation 7 was used. The comparisons are done for modes 1 and 3. This is because these modes are the in-plane modes for which equation 7 is used to calculate (i.e., 2-dimensional modes). Modes 2,4 and 5 are the out of plane modes (i.e., 3-dimensional modes) which equation 7 does not account for. Table 2 also displays the percentage error between the simulation and the analytical calculations.

Table 2: Results of FEA simulations

Analytical	FEA	%Error
118.362	118.54	0.002
N/A	204.32	N/A
739.762	736.03	0.0051
N/A	1246.3	N/A
N/A	2031.7	N/A

In order for the FEA simulation to be considered valid, the frequencies of modes 1 and 3 must be accurate relative to the analytically calculated frequencies. If this is the case then it is assumed that the frequencies for modes 2, 4 and 5 are also correct. It is seen that the FEA simulation can be valid as the largest percentage error is less than 0.1% which means that from an analytical standpoint, the FEA simulation is valid.

3.1.2 Using healthy beam data to create training data to train semi-supervised machine learning algorithm.

Training data is created through the addition of noise. This is done because in practice, the measured frequency response is contaminated by noise. This noise usually impacts the accuracy of the results. Therefore, the FEA data can be used to create a large dataset of noise contaminated frequencies. Each training sample is created by adding random noise to the frequencies obtained from the FEA. The noise is added to each frequency using the following equation (Nhan Nguyen Min, 2010):

$$\omega_{noise} = \omega(1 + n(2rand - 1)) \qquad \textbf{(20)}$$

Where ω_{noise} is the noise-contaminated frequency, ω is the natural frequency, n is the noise level and $rand$ is a uniform random number between 0 and 1. The training dataset is then created using equation 20 in a for-loop. For the generation of data for the numerical investigation, it was decided to go for the lowest possible noise level of 1%. This is to ensure accurate training data to assess if anomaly detection is possible from a numerical standpoint. The code to do this is shown in Abstract B1(Noise code). The dataset created from this procedure is used to train the autoencoder for anomaly detection. Using this method, 1200 noise contaminated healthy beam frequencies were generated.

3.1.2.1. Autoencoder infrastructure:

The autoencoder used for the numerical investigation is a PCA autoencoder. Shown in figure 16. This is an autoencoder that comprises of a PCA algorithm as an encoder and a PCA inverse algorithm as a decoder. The purpose of building this type of autoencoder is because a PCA algorithm, can determine the components within a dataset that have the most variance (and therefore where you should be able to detect anomalies).

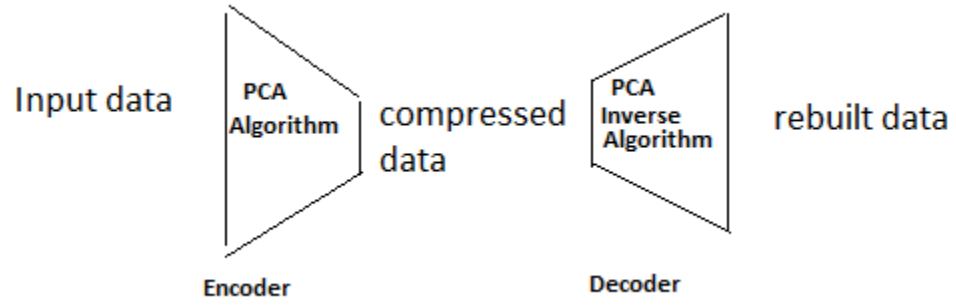

Figure 16: PCA autoencoder infrastructure

The following procedure is followed when creating the autoencoder:

- The training data is fitted to a PCA function. The function is then tasked with determining the principal component where there is the most variance.
- The PCA algorithm then acts as an encoder by taking the first 5 natural frequencies data (5-dimensional space) and reducing it to a lower dimensional space in which the dataset varies the most (i.e., takes data from higher-dimensional space to lower-dimensional space). Figure 17 shows the principal component values. It is seen that more than 90% of the variance is contained in the first 2 principal components. Hence for the numerical investigation, the autoencoder will reduce the dimensionality of the input to 2-dimensions.

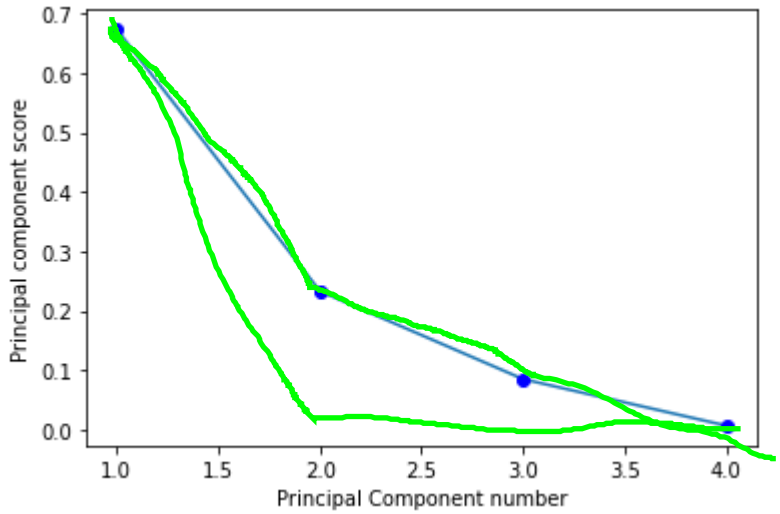

Figure 17: Principal component scores for numerical investigation

The output of this algorithm is the transformed training data (which is essentially the training data transformed into a 1-dimensional space in which the most variance between the data is found). This is how the PCA algorithm acts an encoder.

- The transformed training data is then used as input for the PCA inverse algorithm which takes the output from its 1-dimensional lower space and build it to its original 5-dimensional higher space. Essentially the PCA inverse algorithm serves the purpose of reconstructing, the training data from its compressed form (i.e., the transformed training data). This is how the inverse PCA algorithm acts as decoder.

Appendix B2 contains the code used to build the autoencoder. The idea behind using an autoencoder for anomaly detection is that if the autoencoder is trained using healthy data, it should present larger reconstruction errors when presented with unhealthy data. Therefore, the reconstruction error is used as a way of assessing the validity of the autoencoder. To do this, the mean-squared error was utilised. The mean squared error (referred to as the reconstruction error) of every output sample (compared to its input) is calculated and it is plotted. To create the autoencoder the 1200 samples are split. 900 are used to train the autoencoder and the other 300 are used to test the autoencoder's ability to reconstruct healthy data. Figure 18 shows the results of the reconstruction. It is seen that the 300 samples fall within the reconstruction error range of the of the data that is used to train the autoencoder, therefore it is assumed that the autoencoder can reconstruct healthy data, within a certain error range.

Figure 18: Reconstruction error for healthy beam

3.1.3 Generating vibrational data for cracked/unhealthy beams.

The beam that is analysed for this section has the same properties as is shown in table 1. However, and edge crack a, having non-dimensionalised depth s is inserted along the top of the beam as shown in figure 19. Where s determined by the following equation:

$$s = \frac{a}{T} \qquad \textbf{(21)}$$

This is done for different scenarios in which the edge crack is either made deeper or placed at different positions along the beam.

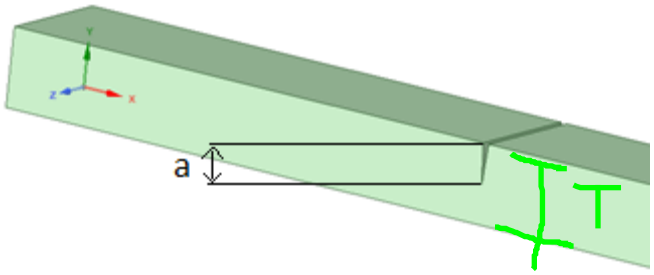

Figure 19: FEA model of Cracked beam

The purpose of doing this is to determine, at which non-dimensionalised crack depth the algorithm starts detecting cracks and to determine at which positions does presence of a crack manifest itself most in the frequencies. These will both be useful for the experimental investigation. There are five different crack scenarios which are considered. Each crack scenario is for when a beam is positioned in the middle of one of five nodes as shown in figure 20.

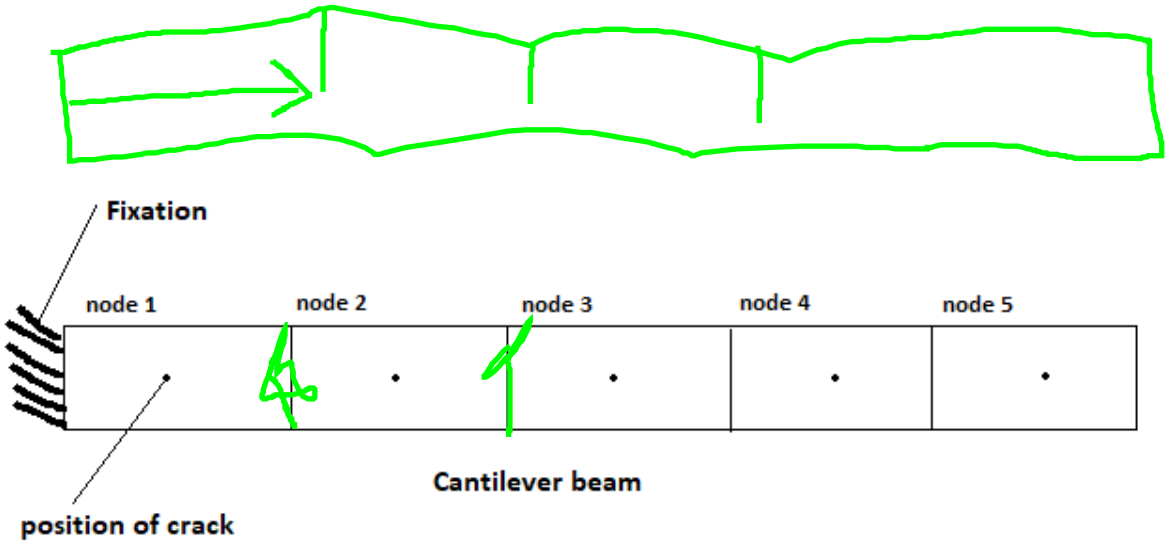

Figure 20: Node setup for cantilever beam modal analysis

Node 1 being the closest to the fixed support and node 5 being the furthest away. At each node, the first five natural frequencies are analysed as the depth of the crack increases as the non-dimensionalised natural frequencies given as:

$$non - dimensionalised\ frequency = \frac{cracked\ frequency}{healthy\ beam\ frequency} \qquad \textbf{(22)}$$

Table 3 gives an example of the non-dimensionalised frequencies at a crack depth of 0.5 for all the nodes.

Table 3: non-dimensionalised frequencies for cracked beams at s=0.5

	Node 1	Node 2	Node 3	Node 4	Node 5
1st	0.86	0.92	0.97	0.92	1
2nd	0.95	0.97	0.99	0.97	1
3rd	0.96	0.98	0.9	0.93	0.99
4th	0.98	0.99	0.97	0.98	1
5th	0.99	0,92	0.99	0.89	0.99
Average	0.948	0.956	0.964	0.938	0.996

What is revealed is that node 1 and node 4 have the lowest average non-dimensionalised frequencies. Therefore, are locations which should be considered for the experimental investigation. It could be possible that these nodes result in the lowest average non-dimensionalised frequencies because they are in positions that affect most of the mode shapes. This is believed to be possible because as one looks at each node (except for node 5 and 2), it is seen that there is a frequency which is the lowest at that node (1st for node 1, 3rd for node 3 and 5th for 4). Therefore, the presence of the crack must affect the mode shape which in turn affects the natural frequency of the beam more.

3.4. First iteration evaluation of algorithm's ability to detect cracks.

The first evaluation technique used to evaluate the algorithm is a visual technique. The performance evaluation of the autoencoder is done in section 3.5. Using the reconstruction error. The reconstruction error of the cracked beams is plotted along with the reconstruction error of the healthy beams and if the a specimen falls within the region of the healthy beams then the specimen

is decided as not being an anomaly (cracked) if it is outside this region, then it is decided as being an anomaly

The frequencies of these beams are used to test the autoencoder for crack depths in the range of 0.1 to 0.5 at each node. Figure 21 (a-e) visualise the results. If the dot is in the blue region, then the

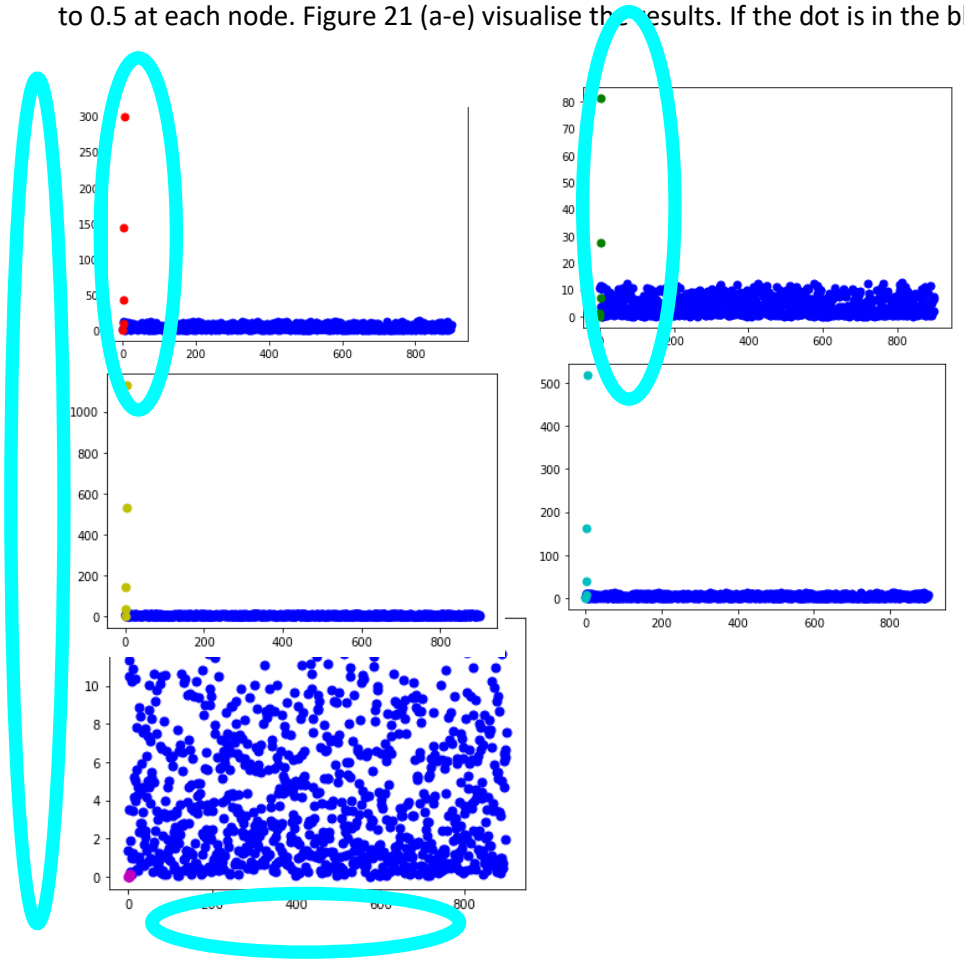

Figure 21: Cracked beam anomaly detection visual a) node 1, b) node 2, c) node 3, d)node 4, e) node 5

autoencoder would have likely not detected the presence of the crack.

If it is outside of the blue region then the autoencoder would have detected the presence of a crack. Table 4 shows the number of times the autoencoder was unable to identify a crack at each node.

Table 4: Number of undetected damage beams

node	No of failures
1	2, s= (0.1, 0.2)
2	3, s= (0.1,0.2,0.3)
3	2, s= (0.1,0.2)
4	3, s= (0.1,0.2,0.3)
5	5, s=all

What is noted from table 3, is that averagely, the frequencies of the cracked beams do not deviate greatly from the frequencies of the healthy beams. With the largest recorded reduction being 14% for a beam that has a crack which is half of its thickness. Therefore, one could imagine that in the presence of noise. It would be quite likely that the autoencoder is going to wrongly evaluate a

cracked beam as being healthy. This is especially the case because this was done with noise levels of 1% which is extremely low. Using standard equipment, higher noise levels should be expected which means it is expected that it will be more difficult to detect cracks.

3.5. Algorithm performance

Because identifying potential damage is a priority in this experiment, a potential solution to this problem would be to decrease the reconstruction error range for which a beam can be considered healthy. This may result in more falsely detected cracks, but more importantly it can also result in the detection of more beams that are cracked. A potential way of evaluating this method is to use the standard deviation. If the mean value of a dataset is known and is presumed to be on a gaussian/normal distribution, any value within 2 standard deviations of the mean is contains 95% of the normal data. If you presume that any value that is outside this range is an outlier than the technique being used is the 2-standard deviation rule (Brownlee, How to Remove Outliers for Machine Learning, 2020). Therefore for this model, a reconstruction error which is higher than 2 standard deviations from the mean will be considered an outlier.

To evaluate the algorithm more test data needs to be generated. This is done in the following manner:

- The damaged frequencies at nodes 1 and 4 will have noise added to them. This is done to evaluate the autoencoders ability to detect damage with noise. The reason why these nodes are selected is because they appear to be the most sensitive to the presence of cracks.
- Healthy frequencies which were not used to train the model will also be used as test data.
- These will be used by the autoencoder, and the following is evaluated:
    - False positives (healthy beams detected as unhealthy)
    - True positives (unhealthy beams correctly detected as unhealthy)
    - False negatives (unhealthy beams which were undetected)
    - True negatives (healthy beams which were correctly undetected)

Procedure:

- Noise is added to the frequencies at nodes 1 -4 for all non-dimensionalised crack depths. Node 5 is left out because the algorithm is not able to detect cracks in this node based on figure 21e.
- Each damage scenario has 15 samples to it. This so that here are an equal number of healthy beams being tested as there are cracked beams being tested.
- The cracked data is fed into the autoencoder algorithm and is reconstructed.
- The mean-squared error values of each sample are determined
- The same procedure is done for the healthy beam test data.
- For this test, an anomaly is characterised as a test specimen that records a mean-squared error value that is 2 or more standard deviations larger than the mean of the training data's average mean squared error (i.e., the 2 standard deviation rule). The 2-standard deviation rule is used as it is suitable for data where the presence of an anomaly does not result in large differences (i.e., the small frequency changes between a cracked and non-cracked beam). Figure 22 visualises how the anomaly detection works, any specimen which records a mean-squared error underneath the red line is seen as being negative (i.e., healthy) and any specimen which records a mean-squared error value above the red line is seen as being positive (i.e., cracked)

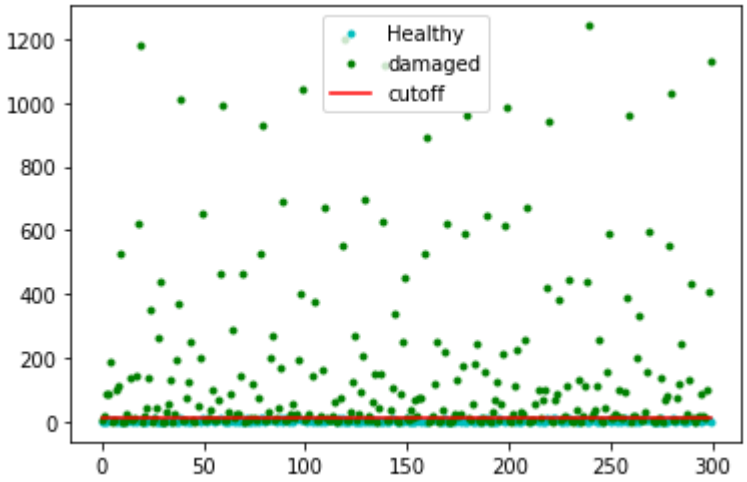

Figure 22: Visualisation of 2-standard deviation rule anomaly detection technique

- The F-measure technique described by equation 19 where B=1. Is used to evaluate the performance of the algorithm. Equation 17 was also used to determine the recall and precision scores. The code for this technique is shown in appendix B3.

The results are shown in table 5.

Table 5: Performance evaluation parameters for numerical investigation

Average Mean-squared error (Training data)	3.92
Standard deviation (Training data)	3.23
Cut-off mean squared error	10.38
Precision score	0.927
Recall score	0.677
F-measure score	0.782

Based on the F-measure score, the algorithm performs at 78.2% when it comes it to correctly determining if a model is cracked or not cracked. These are all calculated and used for equations 17 and 19. To determine the performance of the algorithm in anomaly detection. Using the 2 standard deviation rule, the cracks evaluated in 3.4 are re-evaluated and the results are shown in table 6.

Table 6: Number of undetected damage beams using 2-standard deviation rule.

node	No of failures
1	2, s= (0.1, 0.2)
2	3, s= (0.1,0.2,0.3)
3	1, s= (0.1)
4	3, s= (0.1,0.2)
5	5, s=all

What is seen is that using the 2-standard deviation rule, node 3 becomes more efficient in detecting anomalies.

Things that are revealed from the numerical investigation:

- A PCA autoencoder is able to detect cracks in a structure when using a property of the structure which is inherent to it (namely the natural frequencies). There is a 78% rate of detection for the autoencoder.

- The autoencoder was not able to detect cracks at a non-dimensionalised crack depth of 0.1.
- Nodes of interest which should be considered for investigation in the experimental investigation are nodes 1, 3 and 4.

4. Experimental investigation

The numerical investigation revealed that the autoencoder can detect cracks in a beam using the vibrational data of a cantilever beam. The purpose of the experimental investigation is to evaluate the PCA autoencoder's ability to detect a damaged beam using vibrational data obtained from real-world vibrational experiments as this would be the data that the algorithm would be commonly used for. Experimental investigation includes the following procedures:

1. Setting up experimental modal analysis of healthy cantilever beam
2. Modal analysis of healthy beams and collecting data.
3. Damaging beam and conducting modal analysis of damaged beams
4. Processing of modal analysis vibrational data for autoencoder
5. Using healthy processed vibrational data to train autoencoder
6. Autoencoder performance evaluation

The vibrational data which will be analysed for the experimental investigation is the FRFs. FRFs are chosen as they represent the dynamic behaviour of the structure and not just how the structure behaves at specific frequencies as is the case with the numerical investigation. Also, for practical application an FRF could just be fed directly into an autoencoder instead of having to analyse it and determine things like the natural frequencies.

4.1 Experimental setup

At the university of Pretoria, modal analysis experiments were conducted on a mild steel bar with the following estimated properties (The estimated property being the Young's modulus as the place where it was bought was not able to provide enough necessary information other than it was within the specified range)

Length (L)	475mm
Width (W)	40mm
Thickness (T)	5mm
Elastic modulus	175-200 GPA
Poisson's ratio	0.3
Density	7800 kg/m^3

The experimental setup is shown in figure 23. Where the fixation is the point at which the beam was clamped/fixed, the impact zone is where the beam was impacted by the modal hammer and the

damage zone is point at which an edge crack would be inserted onto the beam.

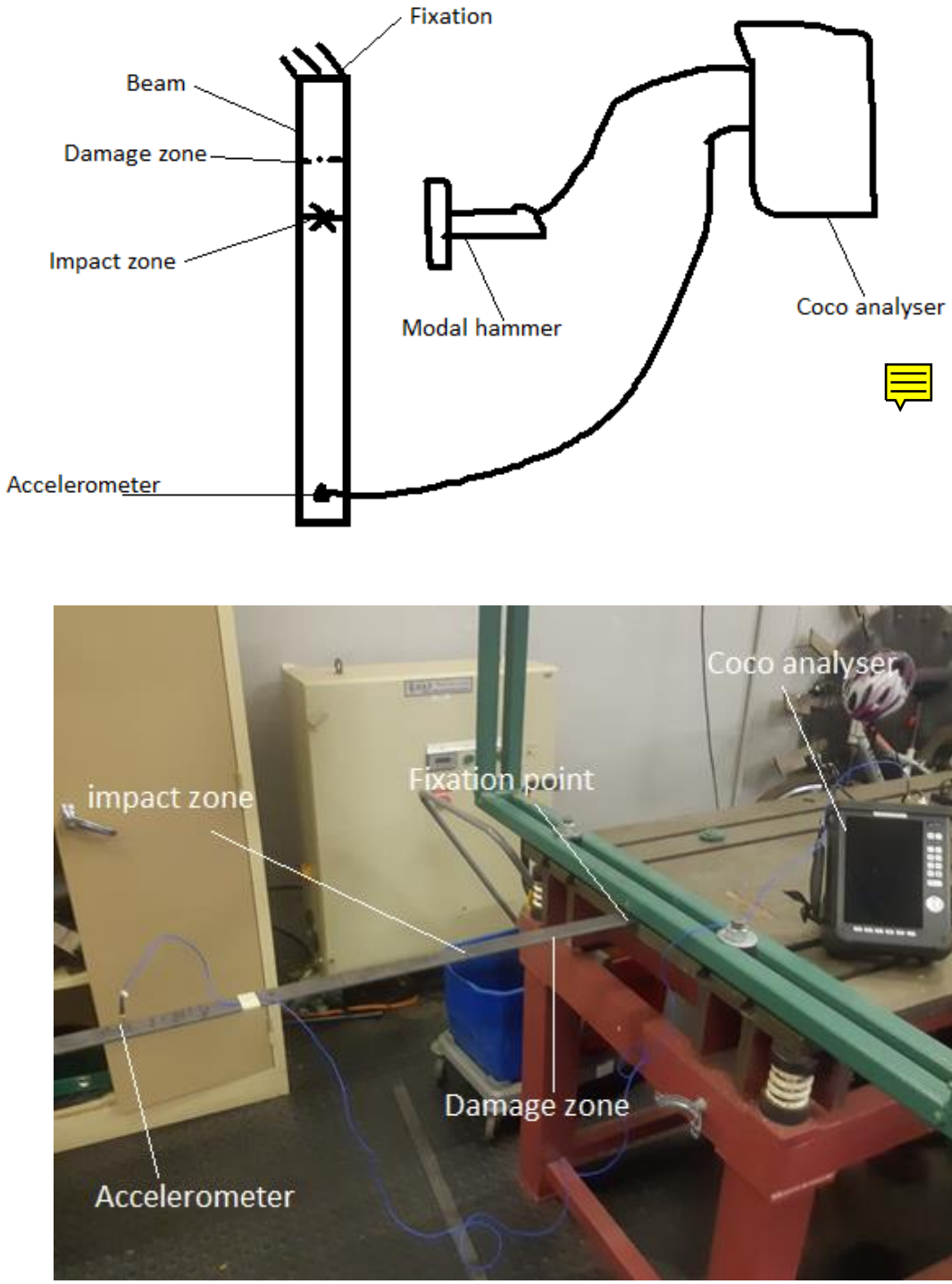

Figure 23: Experimental setup: a) schematic, b) picture diagram

The beam is divided into five nodes as it was in figure 20. This is done to decide where the impact zone, the damage zone and the accelerometer will be positioned. Based on the numerical investigation and Jabbari et al, the best place to position the damage zone is within node 1. This is because the stiffness matrix of the beam is most affected by the presence of a crack in this region and thus impacts the vibrational behaviour of the beam most in this region. The impact zone is decided to be just outside of node 1 as this position is a suitable place to excite the cantilever beam without hitting any nodes whilst also not being too close to the accelerometer. This is validated by

figure in which it is seen that there are no nodes (points at which the displacement response is zero) in the region where the impact zone is expected to be. This also validated by Mr George Breytenbach, who assisted in setting up the experiment. The accelerometer is positioned in node 5 as this region is considered the best place to measure the vibrational response according to Jabbari et al. This is because an accelerometer measures the displacement response of the beam which is its highest near the free end of the beam (seen in figure 15), hence node 5 is the most suitable place to put the accelerometer.

4.2 Healthy beam modal analysis

The first set of experiments conducted were for the healthy beam. The beam is excited by a modal hammer at the impact zone and the accelerometer measures the response. The coco-analyser converts the acceleration response into an FRF. 30 FRFs were generated during the healthy beam

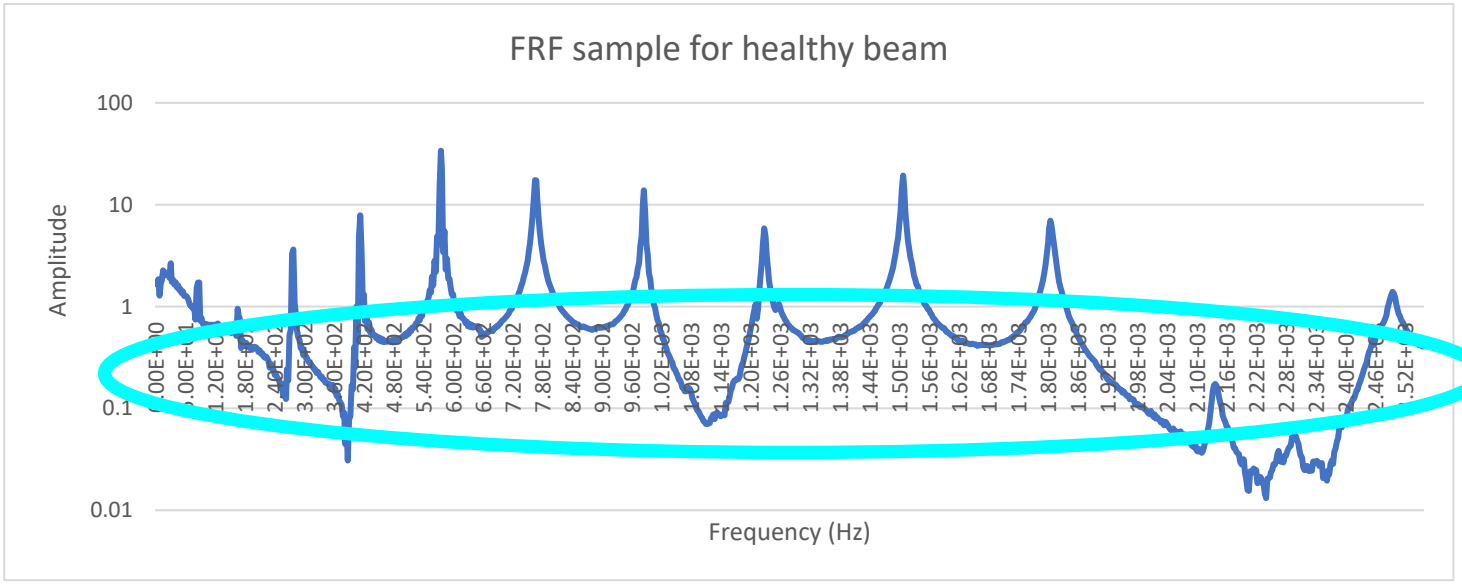

Figure 24: Sample FRF of healthy uncracked beam

modal analysis. A sample FRF is shown in figure 24.

As can be seen from the FRF in figure 24 the beam appears to have 11 natural frequencies under 2 kHz. The presence of so many natural frequencies is utilised in section 4.4 in order to process the training data in a way that may be efficient for the autoencoder to detect anomalies. When compared to the natural frequencies of the same beam when a FEA modal analysis is conducted for a beam with the same properties as the beam used in the experiment (results shown in table 7). It is seen that the natural frequencies do lie within the same regions as many of the peaks within the FRF. Hence it is believed that the experiment can be considered valid.

Table 7: FEA frequencies of healthy experimental beam

1st frequency	17.03 hz
2nd frequency	106.83 hz
3rd frequency	135.11 hz
4th frequency	299.05 hz
5th frequency	377.19 hz
6th frequency	585.95 hz
7th frequency	820.39 hz

4.3 Cracked beam modal analysis

The second part of the experiment was to record FRFs for cracked data. This was done in the following manner:

- Using a saw with 1mm thickness, an edge crack is inserted at the damage zone shown in figure 25.
- An edge crack depth a is inserted at the damage zone as shown in figure.

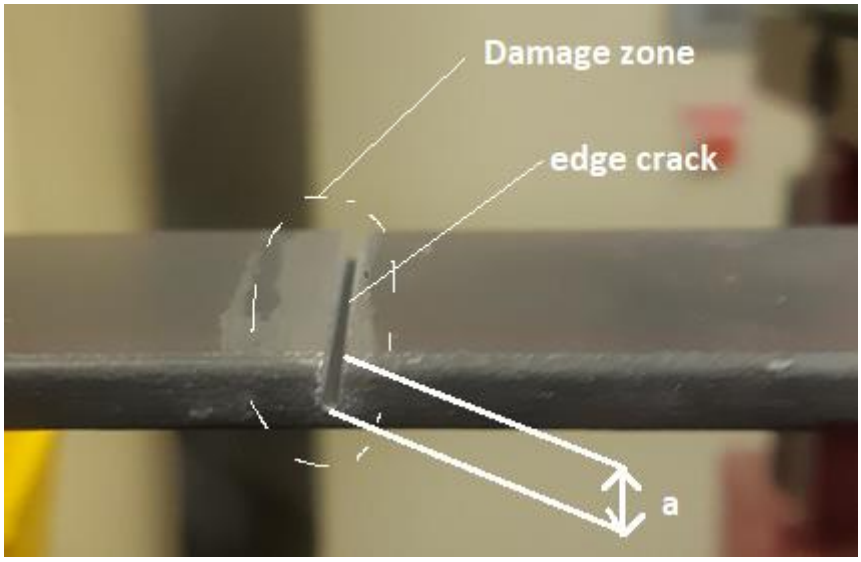

Figure 25: Damage zone of cracked beam used in experimental investigation.

Following the creation of that edge crack. Modal analysis is conducted and FRFs are generated for that crack depth.

- After at least 3-4 FRFs are generated, the crack is increased in order to analyse a new crack depth.
- The non-dimensionalised crack depths analysed are 0.2, 0.4, 0.6 and 0.8. These were chosen as a result of the numerical investigation. Looking at table 4 it was seen that at all nodes, cracked beams were not detected for non-dimensional crack depths of 0.1. With this in mind, it was desired to see if the autoencoder would be able to detect cracked beams with a non-dimensionalised depth of 0.2 and upwards. (This decision is discussed further in section 6)
- Based on research and the numerical investigation, the expected FRF for a cracked beam should look similar to that of the healthy FRF except the peaks should be shifted more towards the left as a result of the decrease in natural frequency. This is shown in figure 26 which displays the FRFs of a healthy beam and a beam with a non-dimensionalised crack depth of 0.8. It is seen that the FRF of the Crack beam does shift to the left. What is also notable is that the amplitude of the cracked beam tends to be higher.

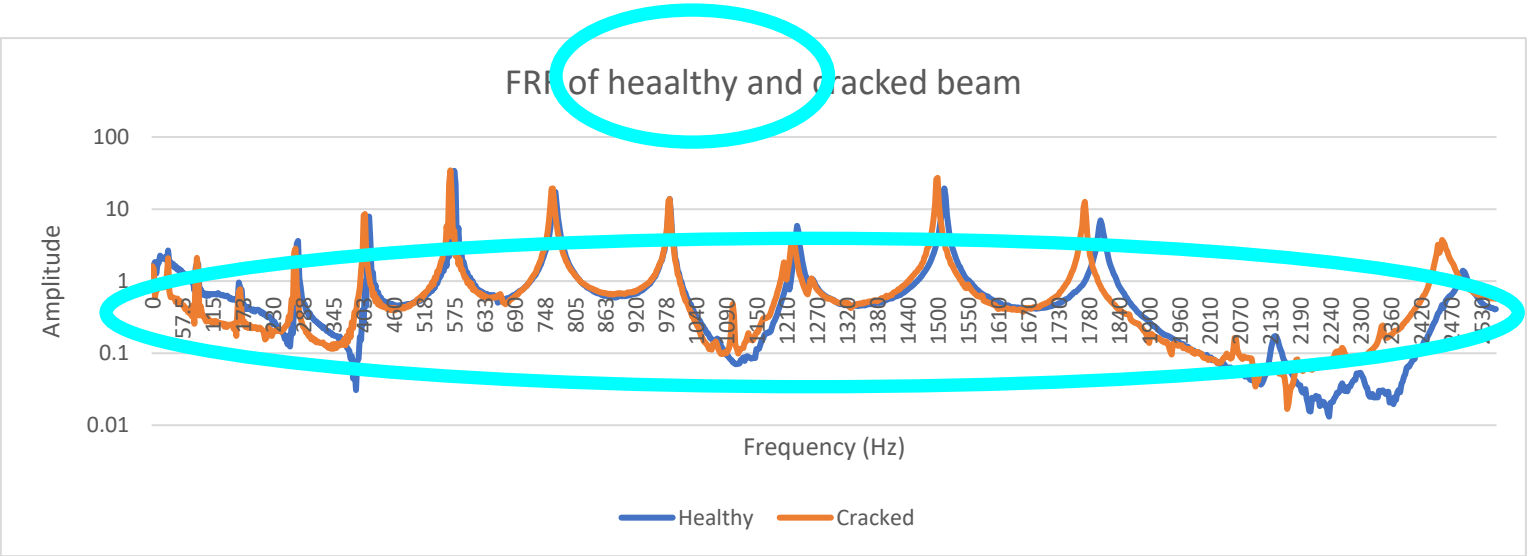

Figure 26: FRFs for cracked and uncracked beam in experimental investigation

4.4 Processing vibrational data for autoencoder

The idea in the experimental investigation is still the same as it was in the numerical investigation (i.e., utilise the reconstruction errors from the autoencoder to detect outliers). The difference now is that instead of using noise polluted frequency values, FRFs will be input. As seen from figure 26 a damaged FRF tends to shift to the left and have a higher amplitude at the resonant frequencies, both these factors should result in higher reconstruction errors if the autoencoder is trained using only FRFs of the beam before it had damage added towards it.

The FRFs are converted into training/testing data in the following way:

- The raw experimental data is processed, the data shows the recorded frequency, the imaginary component of the response and the real component of the response. Equation 9 is used to get the amplitude response. Each FRF is saved into an array.
- Much like the study conducted by Bandara et al (2014), the amplitude array is divided into 4 subsets each meant to capture 2 peaks within them. This is done because the high dimensionality of an FRF can reduce the effectiveness of the PCA for anomaly detection, therefore by dividing the FRF in sub-FRFs the PCA can work more effectively. Also strengthens the system's ability to detect cracks overall, because essentially a specimen is tested 4 times and if it is mis-diagnosed as being healthy in one of the sub-FRFs, it may still be detected as being unhealthy in one of the 3 other sub-FRFs.
- As seen in figure Frequencies under 200hz are not clear, this could be as a result of there being experimental noise or even slight rigid body modes. As a result, they were not used as to ensure accuracy. An example of a sub-FRF is shown in figure 27.

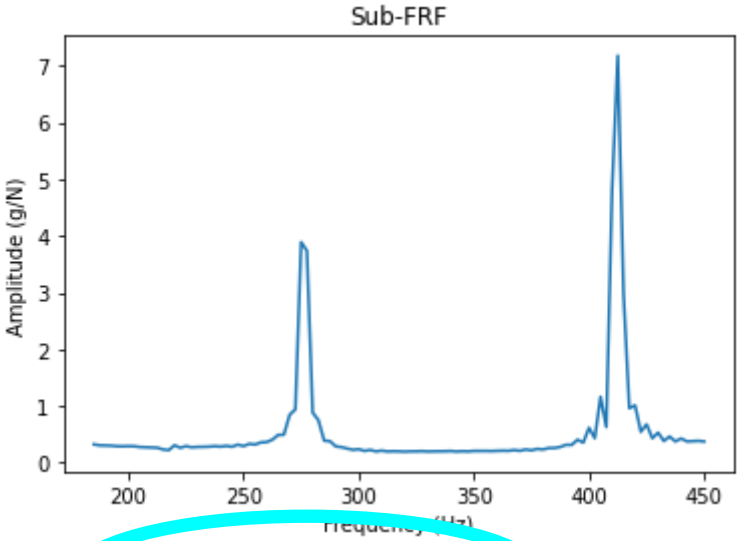

Figure 27: Sub-FRF of healthy beam

4.5 Using healthy beam FRF data to train autoencoder.

The following procedure is used to train the autoencoder (and is also shown in figure)

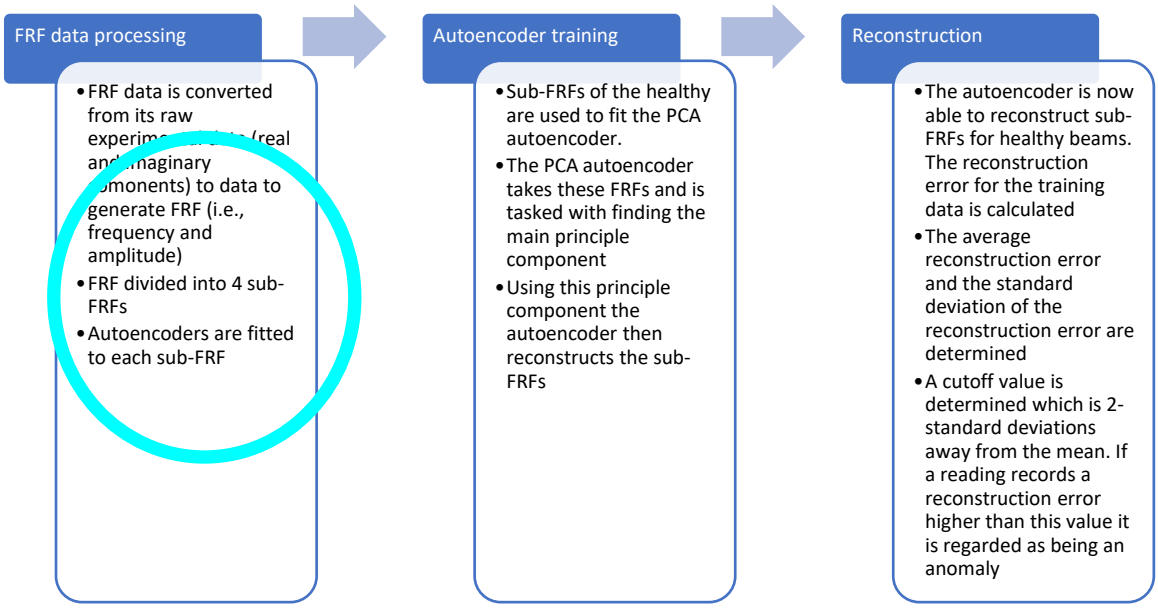

Figure 28: Autoencoder training procedure for experimental investigation

- The 4 subsets are used as input to the autoencoder and the autoencoder reduces the dimensionality down to 1. This done based on the research by Bandara et al, in which the PCA analysis showed that the first principal component contained variance which was significantly larger than all the other principal components this is seen in figure 29.

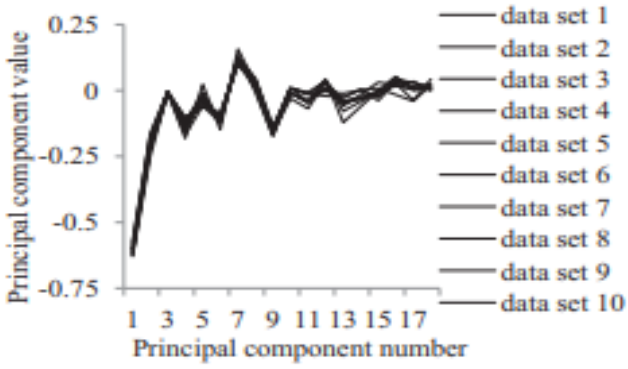

Figure 29: Principal component scores from Bandara et al (2014)

The same analysis is done for the sub-FRFs used in this investigation (shown in figure 30)

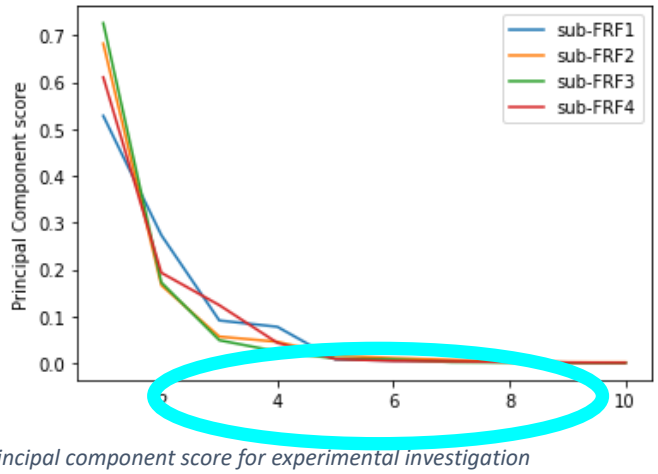

Figure 30: Principal component score for experimental investigation

What is seen is that at the very least, more than 50% of the variance is contained in the first principal component for all the sub-FRFs. Based on this the PCA autoencoder can use the first principal component to reconstruct the FRF data, as it correlates to the principal components shown in Bandara et al (in which majority of the variance is contained in the first principal component). Another thing to note is that the second and third sub-FRFs might be best suited for anomaly detection as the have the largest variances within the first principal component.

- The autoencoder reconstructs the sub-FRF and the reconstruction error of the training data is determined for each specimen trained.
- The standard deviation and average mean squared error is determined. To determine the cut-off, mean-squared error value (using the 2-standard deviation rule)
  The cut-off values are shown in table 8:

Table 8: Cut-off values for sub-FRFs

Sub-FRF1 (Reconstruction error)	Sub-FRF2 (Reconstruction error)	Sub-FRF3 (Reconstruction error)	Sub-FRF4 (Reconstruction error)
0.014	0.026	0.028	0.019

4.6. Autoencoder performance evaluation

The anomaly detection method works in the manner shown in figure 31:

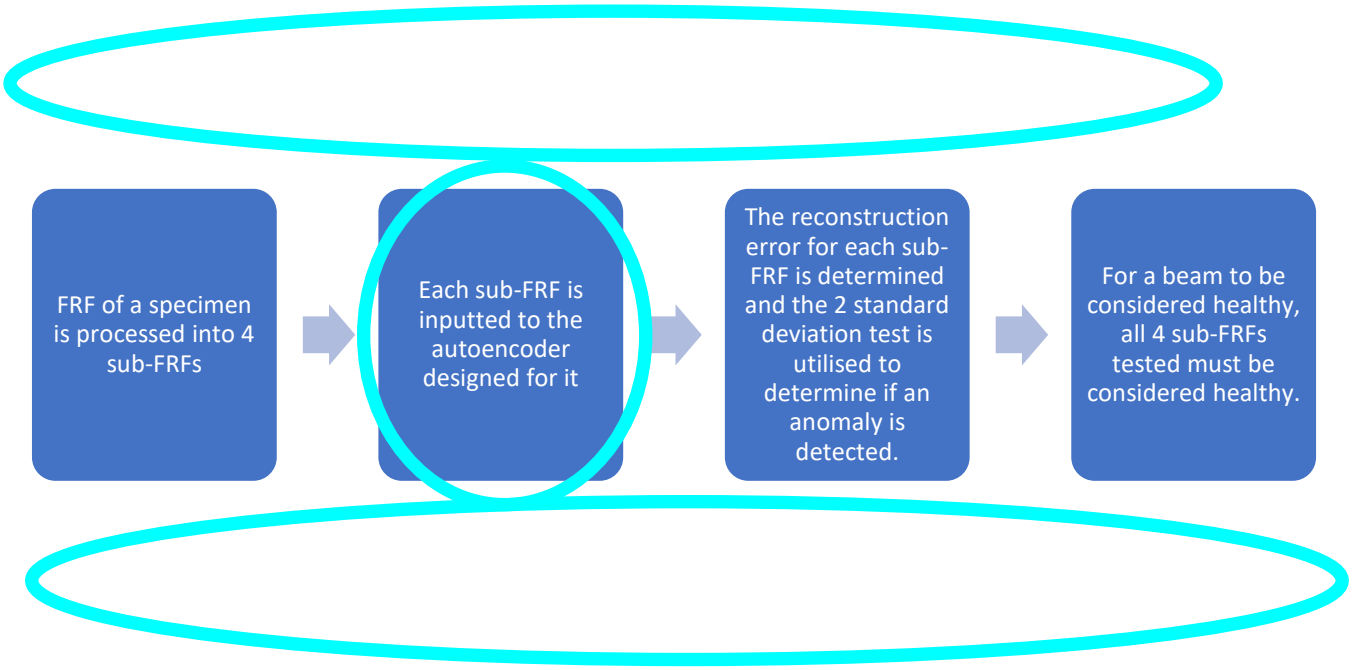

Figure 31: Anomaly detection method flow diagram

The method is now tested using the test data. Test data (which comprises of FRFs of the cracked beams and healthy beams not used to train the model) are used to test the performance of the algorithm. The two standard deviation rule is utilised to detect anomalies. Figure 32 visualises the two standard deviation rule for the experimental test data using the 1st sub FRF.

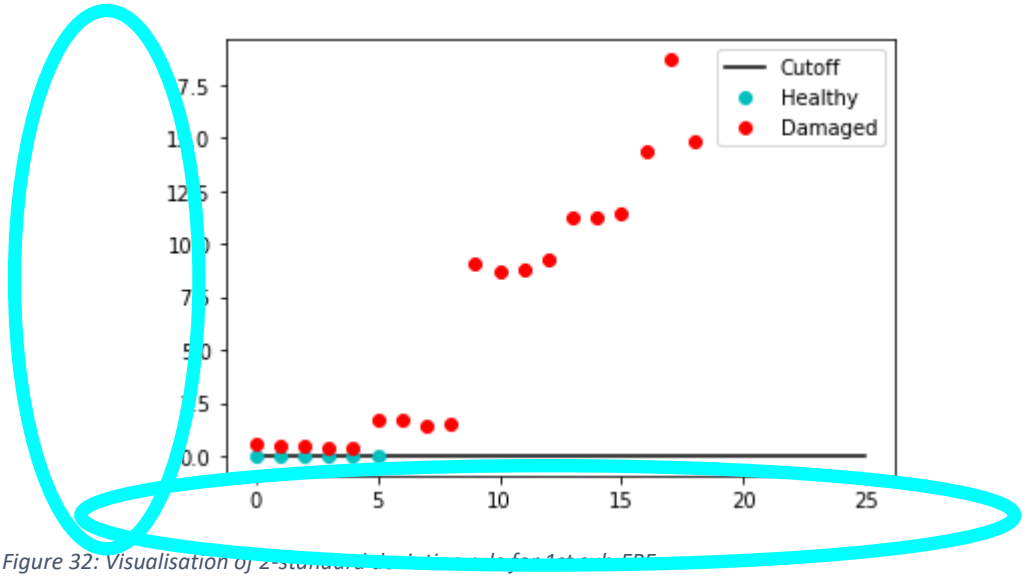

Figure 32: Visualisation of 2 standard deviation rule for 1st sub FRF

As can be seen from the figure 32, it is notable that all the cracked samples will be above the cut-off line.

Table 9:Performance evaluation parameters for experimental investigation

False positives (FP)	0
False negatives (FN)	0
True positives (TP)	19

True negatives (TN)	6
Recall (R)	1
Precision (P)	1
F-measure	100%

Thus, indicating that the model will have a precision score of 1 (as there are no false positives) and a recall score of 1 (as there are no false negatives). Meaning that when the F-measure test is conducted it will result in a 100% performance as seen in table 9.

5. Crack progression method

Sections 3 and 4 shows that it is possible for the autoencoder algorithm to detect cracks on a cantilever beam based on the changes in the vibrational data. The method presented in this section has the aim of trying to evaluate the crack once it has been detected (i.e., to try and see how much the crack has progressed (i.e., determine the non-dimensionalised depth of the crack). The method presented uses the reconstruction error once again to evaluate the depth of the crack. And can be used for the experimental investigations (i.e., when analysing FRFs). The method is essentially an interpolation technique.

To develop the interpolation technique, the FRFs of the damaged beams are used and the average reconstruction error at each non-dimensionalised depth is recorded. This will result in there being an average/expected value at each depth. This shown in table 10.

Table 10: Average reconstruction error values for each sub-FRF

Non-dimensionalised crack-depth	Sub-FRF1 (Reconstruction error)	Sub-FRF2 (Reconstruction error)	Sub-FRF3 (Reconstruction error)	Sub-FRF4 (Reconstruction error)
Cut-off (i.e., 0)	0.014	0.026	0.028	0.019
0.2	0.038	0.45	0.0413	0.26
0.4	0.14	1.59	0.0469	0.73
0.6	1.18	9.97	0.133	3.47
0.8	1.96	16	0.32	9.08

Using this table, the crack can be evaluated in the following way (shown also in figure 33)

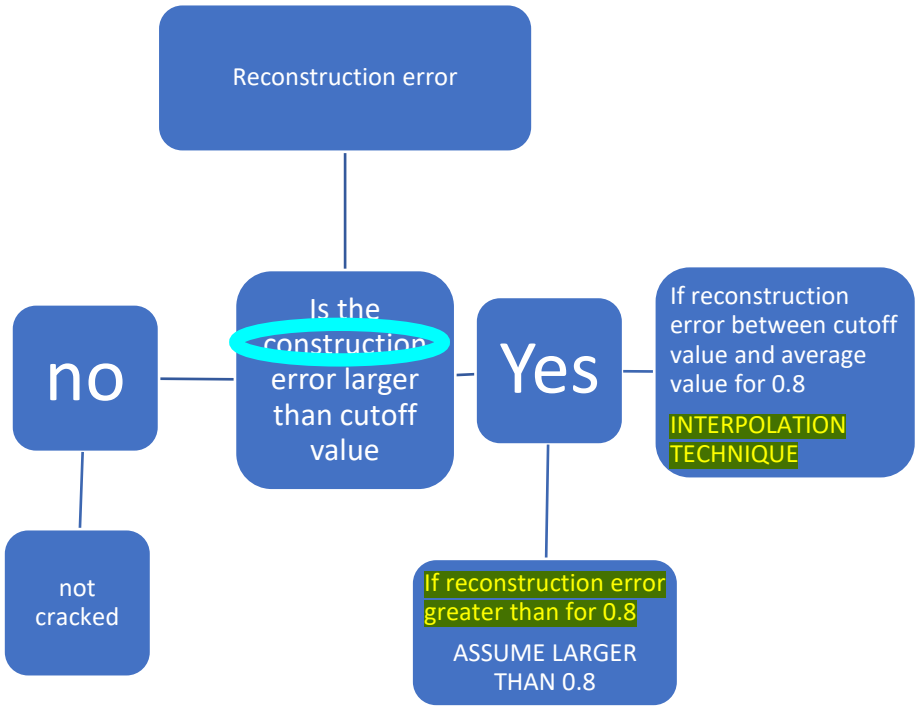

Figure 33: Crack progression procedure

- After a modal analysis is conducted on a damaged test specimen and the FRF has been broken down into the necessary sub-FRFs, one of its sub-FRFs is fed into the autoencoder and its reconstruction error is determined.
- The reconstruction error reveals that the tested specimen is indeed cracked/damaged.
- After a sub-FRF is put into the autoencoder and a crack has been detected, it is expected that the reconstruction error would lie anywhere in the reconstruction errors between the cut-off value and 0.8 (If the reconstruction error is larger than the mean reconstruction error at 0.8, then it is simply assumed that the non-dimensionalised crack depth is larger than 0.8).
- Interpolation can then be used to estimate the size of the crack using the equation 23:

$$s_{estimate} = s_{lower} + (s_{upper} - s_{lower})\left(\frac{Re_{estimate} - Re_{lower}}{Re_{upper} - Re_{lower}}\right) \quad \textbf{(23)}$$

Where $s_{estimate}$ is the estimated non-dimensional crack depth of the observation, s_{lower} is the non-dimensional crack-depth which the observation is believed to be higher than, s_{upper}

is the non-dimensional crack-depth which the observation is believed to be lower than, $Re_{estimate}$ is the reconstruction error of the tested specimen, Re_{lower} is the average reconstruction error for which the specimen is larger than and Re_{upper} is the average reconstruction error for which the tested specimen is lower than.

This can be illustrated in an example. One of the cracked test specimens having non-dimensionalised crack depth of 0.2 is used. When sub-FRF 4 of this specific specimens was input into the autoencoder it returned a reconstruction error of 0.274. Using table, it is believed that the non-dimensionalised crack depth is higher than 0.2 but lower than 0.4 (as it has a reconstruction error larger than 0.26 but smaller than 0.73). The necessary values are then used in equation 24 as shown below.

$$s_{estimate} = 0.2 + (0.4 - 0.2)\left(\frac{0.274 - 0.26}{0.73 - 0.26}\right) = 0.206 \quad \textbf{(24)}$$

6.Conclusions and recommendations

This study aimed to investigate if a data-driven method could be used to detect damaged structures if the data-driven model is trained using healthy data. The study revealed that for a cantilevered beam, the vibrational data would be a possible option to explore. From the numerical investigation it is seen that if a PCA autoencoder is utilised as the data-driven model and is trained with natural frequencies of a healthy cantilevered beam with 1% noise level, the autoencoder performs at 78% for being able to detect cracked beams with a non-dimensionalised crack-depth of 0.1 or higher using the reconstruction error and 2 standard deviation rule (However it must be noted that the algorithm does struggle to detect cracked beams with non-dimensionalised crack depths of 0.1 where there is no noise added to it). For the experimental investigation it is seen that if the PCA autoencoder is trained using FRF data, the autoencoder can detect cracked beams of 0.2 or higher with 100% performance using the reconstruction error and the 2-standard deviation rule. It would also appear that an interpolation technique can be used to evaluate the progress of a detected crack using the reconstruction error.

6.1 Recommendations

The non-dimensionalised crack depths used in the experimental investigation were used because of the numerical investigation (which determined that at a non-dimensionalised crack depth of 0.1, the autoencoder was not able to detect an anomaly by using the reconstruction error. Also, at node 1 it also sometimes struggled to detect cracks for non-dimensionalised crack depths of 0.2). This led to non-dimensionalised crack depths of 0.2 and higher were used and it was seen that the autoencoder did not struggle at all to detect cracked beams. The main difference between the experimental investigation and the numerical investigation is the data that is used. The numerical investigation uses the natural frequencies of a beam, which are inherent to the structure and can only be analysed at certain points whereas the experimental investigation uses FRFs which are dynamic and can be analysed at many points. Therefore, the presence of a crack can change how a whole function changes. Therefore, a crack could possibly be easier to detect for a non-dimensionalised crack depth of 0.1. As a recommendation tests should be conducted on the autoencoders ability to detect cracks for non-dimensionalised depths of 0.1 or lower. Another recommendation is to investigate the ability of this autoencoder to work on structures aside from a cantilevered beam. As the experimental investigation showed, the FRFs of a structure are suitable to detect damage as damage changes the dynamic frequency response of a structure (this logic holds true for all structures and therefore should work for any structure that is used). An advantage of this is that FRF is that it also does not require large amounts of data processing to obtain, and the data needed for an FRF can be easily obtained with the right apparatus.

References

a.i, E. (2020, May 6). *What is Machine Learning? A Definition*. Retrieved from expert a.i: https://www.expert.ai/blog/machine-learning-definition/

Autofem. (2021). *Natural Vibration Frequencies of a Cantilever Beam*. Retrieved from Autofem: https://autofem.com/examples/determining_natural_frequencie.html

Brownlee, J. (2016, May 17). *Crash course on multilayer perceptron neural network*. Retrieved from Machine learning mastery: https://machinelearningmastery.com/neural-networks-crash-course/

Brownlee, J. (2020, August 2). *How to Calculate Precision, Recall, and F-Measure for Imbalanced Classification*. Retrieved from machine learning mastery: https://machinelearningmastery.com/precision-recall-and-f-measure-for-imbalanced-classification/

Brownlee, J. (2020, August 8). *How to Remove Outliers for Machine Learning*. Retrieved from Machine learning mastery: https://machinelearningmastery.com/how-to-use-statistics-to-identify-outliers-in-data/

Cohen, I. (2021). *What is Anomaly Detection? Examining the Essentials*. Retrieved from Anodot: What is Anomaly Detection? Examining the Essentials

Dertat, A. (2017, October 3). *Applied deep learning-part 3: Autoencoders*. Retrieved from towards data science: https://towardsdatascience.com/applied-deep-learning-part-3-autoencoders-1c083af4d798#3f72

developers, G. (n.d.). *Machine Learning Crash Course: Classification: ROC Curve and AUC*. Retrieved from https://developers.google.com/: https://developers.google.com/machine-learning/crash-course/classification/roc-and-auc#:~:text=An%20ROC%20curve%20(receiver%20operating,False%20Positive%20Rate

FCPrimeC. (2019, March). *Why We Need Structural Health Monitoring?* Retrieved from FCprimec: https://www.fprimec.com/why-we-need-structural-health-monitoring

Francesco Trainotti, T. F. (2020). *USING LASER VIBROMETRY FOR PRECISE FRF MEASUREMENTS IN EXPERIMENTAL SUBSTRUCTURING.* Researchgate.

Giosue Boscato, L. Z. (2019). *Structural Health Monitoring through.* Hindawi.

H.Nahvi, M. (2005). *Crack detection in beams using experimental modal data and.*

Johnson, J. (2021). *Anomaly Detection with Machine Learning: An Introduction*. Retrieved from BMC Blogs: https://www.bmc.com/blogs/machine-learning-anomaly-detection/

Leonel, J. (2018, October 29). *Multilayer Perceptron*. Retrieved from Medium.com: https://medium.com/@jorgesleonel/multilayer-perceptron-6c5db6a8dfa3

MechaniCalc. (2021). *Fracture Mechanics*. Retrieved from MechaniCalc: MechaniCalc

Nhan Nguyen Min, V. H.-H.-D. (2010). *A combination of damage locating vector method (DLV) and differential evolution algorithm (DE) for structural damage assessment.*

Nitesh A. Meshram, V. S. (2015). *Analysis of Crack Detection of A Cantilever Beam using Finite Element Analysis.*

P.Gudmunson. (1981). *Eigenfrequency changes of structures due to cracks, notches or other geometrical changes.*

Rao, S. (n.d.). Mechanical vibrations. In S. Rao, *Mechanical Vibrations, 5th edition* (pp. 871-903).

Ray, S. (2017, September 13). *Understanding Support Vector Machine algorithm from examples*. Retrieved from Analytics vidha: https://www.analyticsvidhya.com/blog/2017/09/understaing-support-vector-machine-example-code/

Roylance, D. (2001). *Introduction to fracture mechanics.*

Rupika P Bandara, T. H. (2014). *Structural damage detection method using frequency response functions.*

Shah, T. (2017, December 26). *About Train, Validation and Test Sets in Machine Learning*. Retrieved from towardsdatascience: https://towardsdatascience.com/train-validation-and-test-sets-72cb40cba9e7

Siemens. (2019, November 2). *Natural frequency and resonance*. Retrieved from siemens.com: https://community.sw.siemens.com/s/article/Natural-Frequency-and-Resonance

Siemens. (2020, July 10). *What is frequency response*. Retrieved from Siemens.com: https://community.sw.siemens.com/s/article/what-is-a-frequency-response-function-frf

Trichias Konstantinos, P. R. (2014). *A new approach for structural health monitoring by applying anomaly detection on strain sensor data.*

Tun, J. S. (2018). *Semi-Supervised Outlier Detection Algorithms.*

Yuan, F.-G. (2016). Structural Health Monitoring (SHM) in Aerospace Structures.

Yuequan Bao, Z. T. (2018). *Computer vision and deep learning–based data anomaly detection method for structural health monitoring.* Sagepub.

Yung-Lee, M. G. (2012). *Pseudo Stress Analysis Techniques.*

Appendix A:

List of Symbols

$\sigma^n{}_{i,j}$, undisturbed stress tensor for nth eigenmode

$T_i^n = \sigma^n{}_{i,j} n_j$ traction for nth eigenmode

$u_i^n =$ undisturbed displacement vector for the nth eigenmode

$\varepsilon_{i,j}^n =$ undisturbed strain tensor for nth eigenmode

$\omega_n =$ undisturbed angular eigenfrequency

$f_n =$ undisturbed eigenfrequency

$\sigma_{i,j} =$ disturbed stress tensor

$T_i = \sigma_{i,j} n_j$ disturbed traction

$u_i =$ disturbed displacement vector

$\omega =$ disturbuded angular eigenfrequency

$f =$ disturbed eigenfrequency

$\sigma'_{i,j} = \sigma_{i,j} - \sigma^n{}_{i,j}$

$T_i = \sigma'_{i,j} n_j$

$n_j =$ normal outward vector

$V =$ undisturbed volume

$V' =$ disturbed volume

$C_T =$ part of undisturbed boundary where tractions are equal to zero

$C_u =$ part of undisturbed boundary where displacement are equal to zero

$C'_T =$ part of disturbed boundary where tractions are equal to zero

$E =$ Young's modulus

$\rho =$ density

$W_m =$ strain energy of cut away (material cut out)

$T_m =$ kinetic energy of cut away

$W' =$ corrected strain energy

$W_0 =$ total strain energy

$t =$ thickness of beam

$v =$ Poisson's ratio

$l =$ length of beam

$A =$ amplitude of vibrations

$S =$ cross − sectional area of the beam

$I_x =$ axial moment of inertia

$\lambda_n =$ non − dimensional eigenfrequency

$K_{1M}, K_{1P}, K_{11P} =$ stress intensity factors for rectangular beam with edge crack

1. Perturbation method

The idea of the method is based on the general method to determine the eigenfrequencies of an undisturbed (i.e., no geometrical changes) system which utilize the following solutions to determine the eigenfrequencies and eigenmodes:

$$\begin{aligned} \boldsymbol{\sigma^n{}_{i,j} + \rho\omega_n{}^2 u_i^n = 0} \quad & \boldsymbol{in\ V} \\ \boldsymbol{T_i^n = 0} \quad & \boldsymbol{in\ C_T} \\ \boldsymbol{u_i^n = 0} \quad & \boldsymbol{in\ C_u} \end{aligned} \tag{8}$$

The solution for the undisturbed system is assumed to be known. Equation 8 is then used to model the solution for the disturbed system in which the geometry has changed and has new traction-free boundaries. These solutions are as follows:

$$\begin{aligned} \boldsymbol{\sigma_{i,j} + \rho\omega^2 u_i = 0} \quad & \boldsymbol{in\ V'} \\ \boldsymbol{T_i = 0} \quad & \boldsymbol{in\ C_T{}'} \\ \boldsymbol{u_i = 0} \quad & \boldsymbol{in\ C_u{}'} \end{aligned} \tag{9}$$

For this disturbed system, the eigenmode can be described as:

$$\boldsymbol{u_i = u_i^n + u_i'} \tag{10}$$

Where u_i' is the correction from the disturbed eigenmode to the undisturbed eigenmode. Through combination of equations 8-10 the following solution for the correction u_i' is determined as:

$$\begin{aligned} \boldsymbol{\sigma'{}_{i,j} + \rho(\omega^2 - \omega_n{}^2)u_i^n + \rho\omega^2 u'{}_i = 0} \quad & \boldsymbol{in\ V'} \\ \boldsymbol{T_i' = 0} \quad & \boldsymbol{in\ C'_T} \\ \boldsymbol{u_i' = 0} \quad & \boldsymbol{in\ C'_u} \end{aligned} \tag{11}$$

Multiplying equation 11 with the integral of u_i^n over the volume V' along with the utilization of Gauss theorem, an equation is developed which can determine the unknown angular frequency ω of the disturbed system:

$$\begin{aligned} -\int_{C'_T} \boldsymbol{T_i^n\, u_i^n dS} + \frac{\boldsymbol{\omega^2}}{\boldsymbol{\omega_n{}^2}} \int_{C'_T} \boldsymbol{T_i'\, u_i' dS} \\ + \left(\frac{\boldsymbol{\omega^2}}{\boldsymbol{\omega_n{}^2}} - \boldsymbol{1}\right)\left[\int_{V'} \boldsymbol{\sigma'{}_{i,j}\varepsilon_{i,j}^n dV} + \int_{V'} \boldsymbol{\rho\omega_n{}^2 u_i^n u_i^n dV}\right] = \boldsymbol{0} \end{aligned} \tag{12}$$

To create the first order approximation of ω, the following assumptions are made:

- u_i' is much smaller than u_i^n (reasonable assumption for small geometric changes such as a crack)
- The size of the undisturbed body is of an order of magnitude l and the size of the cutout is of an order of magnitude a and that:

$$\boldsymbol{\frac{a}{l} \ll 1} \tag{13}$$

This is depicted in figure 3

Figure 34: Undisturbed body of size l and volume v with cut out a (P.Gudmunson, 1981)

The rest of the derivation of the formula is available in ref (P.Gudmunson, 1981). However, what essentially happens when these assumptions are made is that a first order approximation can for ω. This approximation takes the form of:

$$\boldsymbol{\omega^2 = \omega_n{}^2 \left[1 - \frac{W' + W_m - T_m}{W_0}\right]} \quad \textbf{(14)}$$

For a system with a small cut being taken out of the material, the volume is essentially unchanged and therefore W_m and T_m are zero. Therefore, the natural frequency of the disturbed system is then described by:

$$\boldsymbol{\omega^2_{cracked} = \omega_n{}^2 \left[1 - \frac{W'}{W_0}\right]} \quad \textbf{(15)}$$

Equation 15 is the important equation that is used to determine the cracked frequency of the system that is used. As the natural frequency and strain energies of a body can be described by different equations depending on the type of body that is being analyzed. In the case of this research topic, it will be a cantilever beam.

To use the perturbation method discussed above, the cantilever must be described as a Euler beam in which the total energy can be described by:

$$\boldsymbol{W_0 = \frac{1}{2} A^2 E \frac{\lambda_n{}^2}{l^4} I_x \cdot l} \quad \textbf{(16)}$$

Furthermore, the natural frequency is described by the following equation:

$$\boldsymbol{\omega_n = \frac{\lambda_n{}^2}{l^2} \sqrt{\frac{EI_x}{\rho S}}} \quad \textbf{(17)}$$

As mentioned in the crack model description of a cantilever beam, when modelling the cracked cantilever beam, the energy of the crack must be considered. For an edge crack, in an infinite half plane with constant stress, the stress concentration factor (K_t) due to the crack is:

$$\boldsymbol{K_t = 1.12\sigma\sqrt{\pi a}} \quad \textbf{(18)}$$

This is used to derive the strain energy of the cracked model by use of the energy release rate equation:

$$\boldsymbol{\frac{\partial W'}{\partial a} = t \cdot \frac{1 - v^2}{E} K_t{}^2} \quad \textbf{(19)}$$

Through integration with respect to a, the strain energy of a cracked cantilever beam is given by:

$$\boldsymbol{W' = t \cdot \frac{1 - v^2}{E} (1.12)^2 \sigma^2 \frac{\pi a^2}{2}} \quad \textbf{(20)}$$

Where the stress σ of a Bernoulli-Euler beam is given as:

$$\boldsymbol{\sigma = \frac{h}{2} EA \frac{\lambda_n{}^2}{l^2} g_n\left(\lambda_n \frac{z}{l}\right)} \quad \textbf{(21)}$$

Where $g_n\left(\lambda_n \frac{z}{l}\right)$ is dimensionless function which describes maximum stress at a point z along the length of the beam. The perturbation method is then applied by subbing equations 16,17,20 and 21 into equation 15. This allows for the natural frequency of a cracked beam to be described by:

$$f^2 = f_n^2\left[1 - 3\pi(1.12)^2(1-v)^2\left(\frac{a}{h}\right)^2\left(\frac{h}{l}\right)g_n^2\left(\lambda_n\frac{z}{l}\right)\right] \quad \textbf{(22)}$$

2. Crack model description

To describe this method the crack model description of the cantilever beam must be understood. This model demonstrates how the presence of a crack influences the strain energy of the beam. Consider a Euler-Bernoulli beam with an edge-crack shown in figure 3

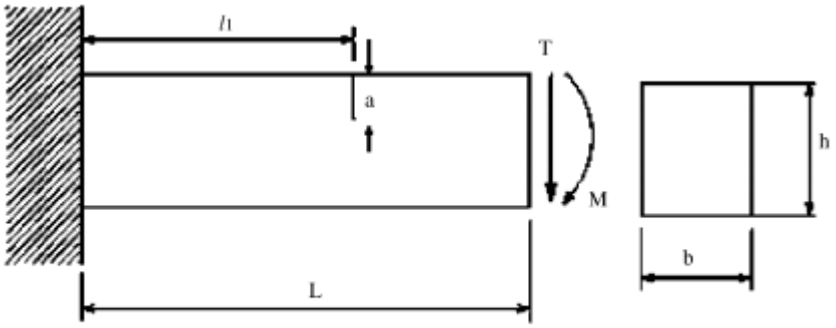

Fig. 1. Schematic model of beam.

3. Figure 35: Euler-Bernoulli beam (H.Nahvi, 2005)

Where L is the length of the beam, l_1 is the distance from the fixed end of the beam to the crack, a is the depth of the crack, T is the shear force on the beam, M is the bending moment on the beam, b is width of the beam and h is the height of the beam. If the beam is divided into elements of length, l then the strain energy U_0 of an uncracked element subjected to a bending moment M_b is given by:

$$U_0 = \int_0^l \frac{M_b^2}{EI}dx \quad \textbf{(2)}$$

Where I is the moment of inertia. The bending moment M_b may be described by the following equation:

$$M_b = Tl + M \quad (3)$$

When the beam is cracked there is additional strain energy. For a rectangular beam with a cross-sectional area of b x h and in state of plane strain, the additional strain energy may given as:

$$U_1 = b\int_0^a \left\{\left[(K_{1M} + K_{1P})^2 + K_{11P}\right]\cdot\frac{1-v^2}{E}\right\}da \quad \textbf{(4)}$$

The flexibility coefficient for the uncracked beam element is described as:

$$C^{(0)} = \frac{\partial U_0}{\partial T \partial M} \quad \textbf{(5)}$$

And the additional flexibility coefficient of the crack is described as:

$$C^{(1)} = \frac{\partial U_1}{\partial T \partial M} \quad \textbf{(6)}$$

Appendix B

B1 training data generation

```
clean_freq=np.array([118.54,204.32,736.03,1246.3,2031.7])
C_n=[]
n=0.01
for i in range(1200):
    rand=np.random.uniform(0,1,size=5)
    newFreq=clean_freq*(1+n*(2*rand -1))
    C_n.append(newFreq)
```

B2: PCA autoencoder

```
Xtrain=C_n[0:900]
xtest=np.array(C_n[901:1200])


from sklearn.decomposition import PCA
from sklearn.preprocessing import StandardScaler
scaler=StandardScaler()
scaler.fit(Xtrain)
pca=PCA(n_components=1)
pca.fit(Xtrain)


X_train_PCA=pca.transform(Xtrain)
X_reconstruction=pca.inverse_transform(X_train_PCA)
xtest_pca=pca.transform(xtest)
xtest_recon=pca.inverse_transform(xtest_pca)
```

B3: Autoencoder evaluation

```
#evaluating autoencoder
cntP=0
cntN=0
for i in range(len(msetestD)):
  if msetestD[i]<10.38:
    cntN=cntN+1
  else:
    cntP=cntP+1
TP=cntP
```

```
FN=cntN


cntP=0
cntN=0
for i in range(len(msetestH)):
  if msetestH[i]<10.38:
    cntN=cntN+1
  else:
    cntP=cntP+1
FP=cntP
TN=cntN


P=TP/(TP+FP)
R=TP/(TP+FN)
B=1
Fmeasure=((1+B**2)*R*P)/((B**2)*(R+P))
print(Fmeasure)
```

Appendix C: RPP

Data Driven automatic damage detection model for cantilevered beam

MRN 422 Research Project Proposal

Inkanyezi Pascal
170555459

Project summary

The purpose of this research task is to develop an automatic damage detection model (structural health monitoring system) for cantilevered beam using data-driven models. This model must then be able to determine if a structure is damaged based on measured vibrational data of a cantilevered beam.

Background

The research project is specially focused on 3 areas, discussed below:

-Structural health monitoring (SHM) are automated methods for determining changes in structural integrity of mechanical systems. SHM serves to provide assessment of a structures ability to perform its task and is therefore useful in civil, military and aerospace engineering applications [1]. An SHM system typically consists of diagnosis component which consists of damage detection and a prognosis component which assesses and determines consequences of the diagnosed damage. SHM is important because capital intensive assets/structures need cost-effective and reliable monitoring and inspection techniques which ensure the integrity and reliability of these structures. SHM systems can offer these solutions when combined with non-destructive testing (NDT) solutions [2]. An example of this is seen in a study of existing structures in North America which are approaching the end of the design service life. It is reported that approximately 56000 bridges are structurally deficient and thus vulnerable to failure. Implementation of SHM systems aid in detecting the ways in which such structures are vulnerable and help maintenance engineers determine how to mitigate/eliminate vulnerabilities of existing structures. Thus, prolonging the service life of the structures. For these reasons, SHM is an important concept in engineering, which is why the development of an SHM model is investigated for this research topic.

As mentioned before, SHM is efficient when coupled with NDT solutions. The NDT method utilised in this research topic is modal analysis.

-Modal analysis is a technique that is used to determine the vibration characteristics (mainly natural frequencies and mode shapes) of a mechanical structure or component undergoing vibration [3]. The natural modes and frequencies of vibration are inherent to the structure and can therefore be used to determine its physical properties. As a result, modal analysis is commonly used as form of non-destructive testing for structures.

This is useful for SHM because when a structure has a crack, a local flexibility is introduced which changes vibration response of the structure [4]. By comparing the vibration response of a healthy structure to that of a cracked structure, the position, depth and other characteristics such as stress concentrations can be determined.

As mentioned before, the SHM is created using data driven models. Therefore, machine learning is deemed to be useful tool in the development of the SHM model.

-Machine learning is a data analytics technique used to teach computers to learn from experience with the experience coming in the form of data/ information. It is a form of artificial intelligence

capable of providing a system with the capabilities to automatically learn and improve from data/experience without explicitly being programmed to do so.

Machine learning is useful for SHM as it offers the ability to rapidly analyse the relationship between data variables and generate outputs. Machine learning also offers faster computing time for problem solving. These factors deem machine learning to be a useful tool for development of automatic systems such as that of an SHM system.

Objective and Scope

The purpose of this research is to develop an automatic damage detection system for a cantilevered beam using data driven models. This is an SHM system that is created through the utilisation of vibrational analysis techniques as well as machine learning techniques to drive it. The idea is that this SHM system is an anomaly detection system, in which the anomaly is a cracked. Overall, there are two objectives aiming to be achieved through this system. The primary objective is to develop the diagnosis component of the SHM system which must be able to determine if there is a crack on the cantilever beam. The secondary objective is to develop another aspect of the diagnosis component. This aspect of the component aims to evaluate the crack in terms of position and depth. The purpose of this component is to help the user evaluate whether the structure is suitable for operation based on the requirements they might have for the structure (i.e., from the evaluation results of the prognosis component, the user can assess things such as potential stress concentrations that the structure may be exposed to and from that decide if it suitable for safe operation).

The diagnosis component utilises finite element model simulations, analytical and numerical procedures as well as machine learning techniques to develop a method of crack detection. This model will then be tested on simulated data of beams that would contain the anomaly (which would be a crack). It is then evaluated using vibrational data obtained from physical vibrational analysis experiments of cantilevered beams. The second aspect of the prognosis component will utilise numerical and analytical methods to process the data and determine the position and depth of the crack. For this project to be completed, an array of subtasks needs to be performed. The tasks to be performed include the following:

- Numerical investigation (primary)
    - Development of Diagnosis component:
        - Finite Element model (FEM) modal analysis simulations of cantilever beams
        - Development of numerical/analytical procedure for crack detection in beams
        - Testing of diagnosis component using data with anomalies
- Experimental investigation
    - Diagnosis component testing
        - Physical Modal analysis experiments of cantilever beams
- Numerical investigation (secondary)
    - Development of prognosis component
        - Development of numerical/analytical procedure used as prognosis component of SHM system.

Procedure:

The proposed procedure for developing the SHM system for this research project will consist of the following:

- Numerical investigation
  - Development of diagnosis component: Data acquisition system-Modal analysis (FEM and simulation automation):
    FEM pre-stressed modal analysis simulations of non-cracked cantilevered beam model will be conducted and the FEM software to be used is ANSYS. From the simulations, the vibrational data are recorded. The simulations serve two purposes. Firstly, the simulations will be the primary source of data which is processed and is used to train the SHM system's machine learning algorithm. Secondly, the simulations are compared with the experimental results for validity purposes.
    When performing the FEM simulations, the following procedure will be completed in Ansys:
    - A Beam specimen with the same geometric and material properties as those used in the experiment are created
    - The beam is given fixed support boundary conditions on one end and free boundary conditions on the other end. This is done to replicate the boundary conditions of a cantilevered beam.
    - The relevant vibrational data is recorded.

    The process is then automated using programming software to create large amounts data to use to be utilised in the algorithm's training. A large amount of FEM samples need be generated from these simulations and randomised samples can be created using techniques such as Latin hypercube sampling.

  - Development of diagnosis component: Data processing system- The automated data python is processed. The idea is to take variables for each sample generated through the FEM simulations (such as elastic modulus, Poisson's ratio, natural frequencies etc.) and convert them into variables which would aid in developing a numerical/analytical procedure to for crack detection based on vibrational data (the variables needed for this procedure will be determined through research). After the data is processed and the procedure for crack detection has been established. The data will be fed into a machine learning algorithm. The machine learning algorithm will be one best suited to anomaly detection and will be determined through research. The machine learning algorithm will be created using Python as this is a very suitable programming language for machine learning.

  - Testing of diagnosis component: Cracked FEM models:
    In the same way that the non-cracked FEM models were generated, Cracked cantilever beam samples will be generated. These samples are then used as testing data for the diagnosis component to test if the diagnosis component can detect a cracked specimen.

- Experimental investigation

  - Testing of Diagnosis component- vibrational analysis (experimental).

Vibrational analysis of a cantilevered beams will be conducted physically at the University of Pretoria. 2 beams will be used, with one beam having no cracks/damage and the other beam having cracks/damage. The purpose of these experiments is to create data vibrational data which will be used to evaluate the diagnosis component's(which is component created purely from FEM data) ability to analyse real-world vibrational data that has practical issues such as news. The beam having no cracks is used to validate whether the diagnosis component can determine when a beam is healthy (i.e., has no crack detection) and the cracked/damaged beam is used to validate whether the diagnosis component can determine if the beam has a crack. At this point it is important to note that what constitutes a cracked beam would be a beam that is still able to be place in a cantilevered position without experience mechanical failure, but the crack is large enough that the vibrational data would deviate from the expected behaviour of a non-cracked cantilevered beam (research will need to be conducted to determine the exact specifications of a cracked beam) From these experiments the vibrational data of the specimen will be recorded.

The data extracted from these experiments will be the vibrational data. These are used to determine the natural frequencies and mode shapes of the cantilevered beam. The data will then be processed for the SHM system to interpret it. Research needs to also be conducted as to which type of vibrational analysis is best suited to cantilever beam vibration.

- Crack progression (secondary)
    - Development of Prognosis system: Structural health evaluation- The prognosis component aims to evaluate a cracked beam depth of the crack. This will be done using numerical procedures and analytical equations that will be determined through research (e.g., the perturbation method). Research will also be done to determine if the prognosis component can be improved by the implementation of machine learning algorithms.

The success of the system is judged on the following conditions:

- Primary condition: The diagnosis component is able to detect if a beam specimen is damaged (i.e., damage detection)
- Secondary condition: The diagnosis component can determine the depth of cracks

The SHM system is considered successful if the primary condition is met.

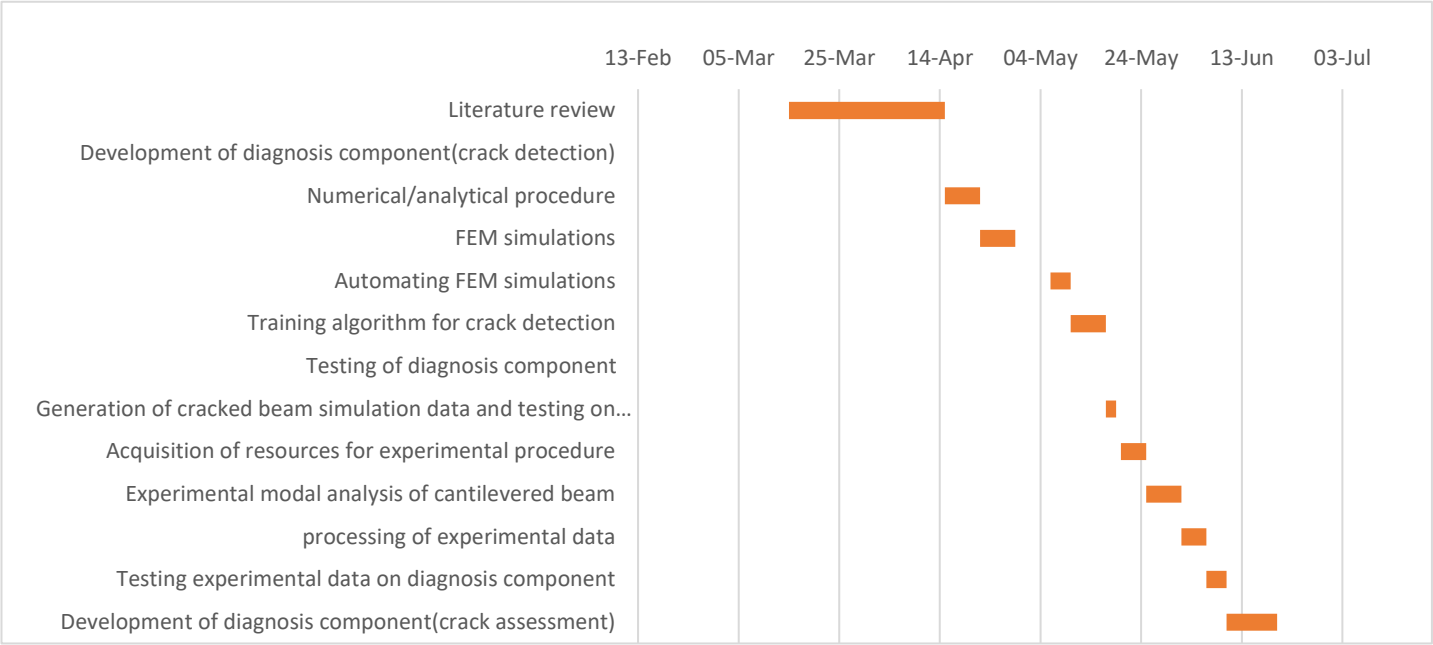

The Gantt chart for the tasks is shown below:

References

1. Sciencedirect- Structural Health Monitoring. 2020. Available at: https://www.sciencedirect.com/topics/engineering/structural-health-monitoring
2. FPrimeC Solutions Inc. 2021. Why We Need Structural Health Monitoring? Available at: https://www.fprimec.com/why-we-need-structural-health-monitoring
3. Sciencedirect- Modal analysis. 2020. Available at: https://www.sciencedirect.com/topics/engineering/modal-analysis
4. H. Navhi, M. Jabbari -Crack detection in beams using experimental modal data and finite element model. 2005